THE MECHANICAL DESIGN OF A PASSIVELY ADAPTING EXOSKELETON FOR THE LOWER ARM

April 3, 2011

Wouter H. Broeze[1,2]**, Just L. Herder**[1]
[1] Delft University of Technology
Faculty of Mechanical, Maritime and Materials Engineering
Department of BioMechanical Engineering
Delft, The Netherlands

Emile J. Rosenberg[2]
[2] InteSpring B.V.
Delft, The Netherlands

ABSTRACT

Lifting patients is a demanding task for care providers. In addition, the number of patients is rising and the number of people with obesity is expanding. Current lifting aids are single purpose and time consuming to use. Exoskeletons can fulfill the demand for a versatile and easy to use lifting aid. A drawback of a typical exoskeleton is that in order to function correctly the axes need to be aligned to the human joints, which is time consuming. Furthermore, an exoskeleton for healthcare must reduce the reaction forces in the user while lifting. It is chosen to design an exoskeleton, which requires no adjustment and can cope with power enhancement. The goal of this paper is to design an exoskeleton that is fast, easy to use and reduces the reaction forces in the user. A design is proposed which easily fits different sized users. In addition the reaction forces in the human skeleton are eliminated. The model is tested by means of a demonstrator. Elastic tension elements are used as a gravity compensator. By reducing the potential energy fluctuation the required external input is reduced. Optimizing a number of design parameters leads to a calculated moment reduction of 98.8% and moment fluctuation reduction of 96.8%. This is the first exoskeleton to combine fast to use design with high-energy efficiency gravity compensation.

Keywords: exoskeleton, passive adaptation, power enhancement, lifting aid

1 INTRODUCTION

The demand for healthcare is growing. The number of patients will rise substantially the coming years [1]. Furthermore, the number of people with obesity is expanding. This implies a need for lifting mechanisms to assist the care providers. Current lifting mechanisms are single-purpose and time consuming to use. Robotics, in particularly exoskeletons can fulfill the demand for a versatile and easy to use lifting mechanism. With the use of exoskeletons in healthcare to assist the care provider, the quality of healthcare can be maintained with fewer people [2].

To create a new lifting aid it is chosen to focus on an upper-body exoskeleton to assist the care provider. Exoskeletons can be used more versatile than current lifting aids. In addition, exoskeletons follow the human movements.

There are three prominent applications for exoskeletons; rehabilitation [3,4], teleoperation [5] and power enhancement [6]. Assisting a care provider to lift a patient is considered as power enhancement. Therefore the exoskeleton must be competent for power enhancement.

A drawback of a typical exoskeleton is that in order to function correctly, their axes need to be closely aligned to the anatomical axes of the human joints. Without correct alignment the exoskeleton can feel uncomfortable and create reaction forces in the human joints [7,8]. For an exoskeleton to be successful in healthcare it must be fast to use. To align a typical exoskeleton for usage can take 5 to 15 minutes [4] which is too long.

To align the exoskeleton to the human joints is difficult because the anthropometrics differ between people. Moreover, human joints are seldom simple hinges. In addition, the exact locations of the human joints are difficult to determine without the help of imaging devices. Even when the setting for previous usage are saved, final adjustment is required before every usage [9].

We propose to design an exoskeleton which requires no active alignment adjustment and can cope with power enhancement. This design combines the easy to use benefit of an exo-

skeleton with the strength of a current lifting mechanism. This design can also be used to assist the care provider in other demanding tasks in healthcare.

Current exoskeletons have different approaches for solving joint misalignment. For example, the DAMPACE [10] and the exoskeleton of the European Space Agency [7] require no joint alignment. This is achieved by making the exoskeleton passively adapting. However the DAMPACE is designed for rehabilitation and the European Space Agency exoskeleton is designed for teleoperation. Both systems are not capable to be used as a power enhancement exoskeletons, since both systems rely on the human skeleton to counteract the load forces.

The first goal of this paper is to design the mechanical part of an exoskeleton for the lower arm which requires no active joint alignment. The second goal is to reduce the reaction forces in the user caused by the load.

This paper will have the following structure. Section 2 will discuss the method used. In Section 3 the conceptual design is addressed. An analytical model and evaluation of the final concept are discussed in Section 4. Section 5 will address the demonstrator build. In Section 6 an optimization for gravity compensation is addressed. Section 7 contains the discussion and the conclusions are presented in Section 8 .

2 METHOD

A method was adapted [11] and used to design a mechanical system which realizes the design goals. For this project a number of assumptions were made.

- The system was evaluated in the two dimensional plane.
- One arm was evaluated.
- A limited range of motion was chosen.
- It was assumed that the shoulder and elbow joints are simple hinges, because of the 2D plane assumption combined with the limited range of motion.
- The system was analyzed in a quasi-static fashion. A quasi-static analysis is based on the assumption that the kinetic energy changes and dynamic forces are negligible compared to the potential energy changes and the static forces. Additionally a quasi-static system is regarded as time independent, which makes calculation of every individual position possible.
- No action was taken in designing the connection between the user and the system. Only the function of the connection was assessed.

2.1 Function

For this paper a lifting motion was chosen as design case. A functional case is assessed in which the care provider lifts a patient in a lying position from a bed to a shower bed. Following are the steps in this design case.

1. Care Provider (CP) sets up the shower bed and the Exo-Skeleton (ES)
2. CP puts on the ES
3. CP activates the ES
4. CP places his/her arms with the ES underneath the patient
5. CP lifts the patient
6. CP rotates to the shower bed
7. CP lays down the patient
8. CP removes his arms from underneath the patient
9. CP deactivates the ES
10. CP takes off the ES

One of the design goals was to design a system that fits different users. This goal returns in step 2 of the function description. Step 4 implies a compact design. If the system is too large, it obstructs the movement of the care provider. Furthermore, step 4 gives an indication of the range of motion needed for this design case. In step 5 the weight of the patient is in the arms of the care provider. Here, the corresponding reaction forces in the user needs to be reduced.

2.2 Requirements

For the system to function properly as a lifting aid, it needs to fulfill a number of design requirements.These requirements follow from the design case. Figure 1 shows a schematic representation of a human arm with the essential parameters. Tabel 1 summarizes the values of the requirements.

The first two requirements were based on the fact that the exoskeleton must not constrain the users movements (function steps 4 and 8). For the shoulder a small range of motion (θ) is sufficient $[\frac{\pi}{4} : \frac{\pi}{2}]$. The elbow (γ) is rotated more during lifting and requires $[0: \frac{\pi}{2}]$.

The third requirement involves the reaction forces in the user (function step 5). For low frequency lifting tasks without a lifting aid a load of 23 $[kg]$ is accepted [12]. Therefore the maximum reaction force in the user was selected at 115 $[N]$, since this paper focusses on one arm.

The fourth and fifth requirement concern the difference between the users (function step 2). Every person has different anatomical properties. Allowing the majority of the population to use the system is a key feature. The P05-P95 norm was used to determine the range of adjustment needed. The upper arm varies between 0.295-0.398 $[m]$ and the length from the elbow to the hand palm ranges between 0.297-0.385 $[m]$ [13].

The sixth requirement involves the space below the lower arm (function steps 4 and 8). Lifting a patient requires the user to move his arm underneath the patient. This invokes the need for a compact system. Extending the hand to its limit position, the perpendicular distance from the fingertips to the center of the lower arm is approximately 0.12 $[m]$. This was chosen as the design space for the lower arm. There are no hard restrictions set for the design space around the upper arm.

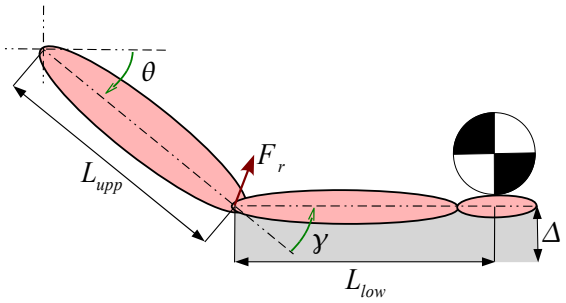

FIGURE 1: *2D schematic representation of a human arm. The range of motion of the lower and upper arm, position of the reaction force, the load and the design space of the lower arm are indicated. The gray area underneath the lower arm is the space the exoskeleton is allowed to occupy. For the upper arm no hard limitations are set on the design space. In Tab. 1 the values of the given parameters are listed.*

TABLE 1: *Design requirements for the mechanical system. RoM stands for Range of Motion.*

	Parameter	Quantity	Unit
RoM Shoulder	θ	$[\frac{\pi}{4} : \frac{\pi}{2}]$	*rad*
RoM Elbow	γ	$[0: \frac{\pi}{2}]$	*rad*
Max Reaction Force User Joint	F_r	115	*N*
Length Upper Arm [13]	L_{upp}	[0.295-0.398]	*m*
Length Elbow to Palm [13]	L_{low}	[0.297-0.385]	*m*
Design Space	Δ	0.12	*m*

In addition to these hard requirements there are a number of soft requirements. These indicate the characteristics of an ideal system. It is preferred to have a light, compact, cheap and simple system with minimal movement restriction to the user. It is preferred to use elastic elements for gravity compensation.

3 CONCEPTUAL DESIGN

The design method explains the general design steps. In this section the generation, analysis and the evaluation of the concepts are addressed in the corresponding sequence.

The concepts are constructed out of a number of basic elements. The function of these basic elements are indicated. Table 2 lists a number of basic elements.

Although these basic elements and their functions are generally acknowledged, this breakdown provides a structural method to generate concepts. Most element functions can be achieved by the combination of other elements in a certain way. This approach is used to create new concepts and to eliminate the weaknesses of others. Figure 2 displays four concepts.

TABLE 2: *Basic elements with their key function. All elements listed here are used in the concepts shown in Fig. 2.*

Element	Function
Link	Rigid connection between two or more points inline
Joint	Locks the two translation DoF between two ore more elements
Body connection	Creates connection between the user and the system
Extension Spring	Affects force depending on its elongation
Linear guide	Allows one translation and prevents other DoF
Cable	Can only transfer tensile force
Pulley	Guides a cable around a constant radius

3.1 Analysis

During the analysis of the concepts a difference of adjustment is found. The concepts are divided into three categories.

System adjustment
These concepts adjust to the user by changing the complete geometry.
Hinge adjustment
These concepts adjust the geometry of the hinge to adapt to the user.
No adjustment
The system is designed to fit all users without changing the system.

Concept I (Fig. 2a) uses system adjustment. The benefit of this type of adjustment is that the whole system works to adapt to the user. This implies a smaller system as a drawback, when the system is scaled, the adjustment range also changes. Concepts II and IV (Fig. 2b, 2d) are categorized as hinge adjustment. An advantage of this adjustment is that the hinge can be used as an add-on to existing exoskeletons. However, achieving a large ad-

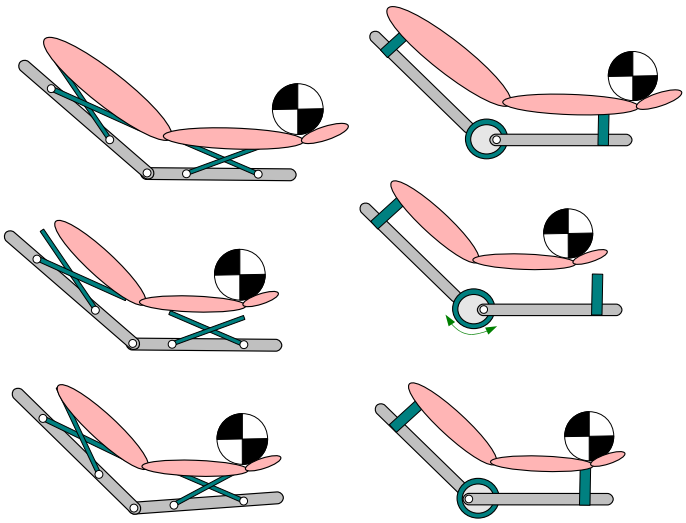

(a) Concept I

(b) Concept II

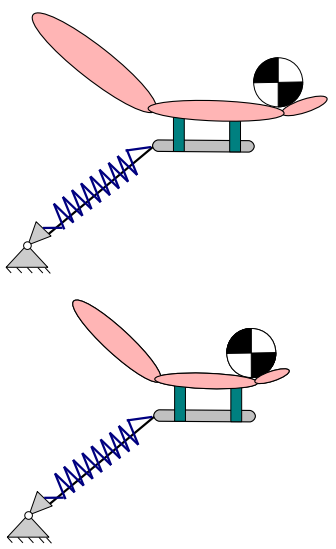

(c) Concept III

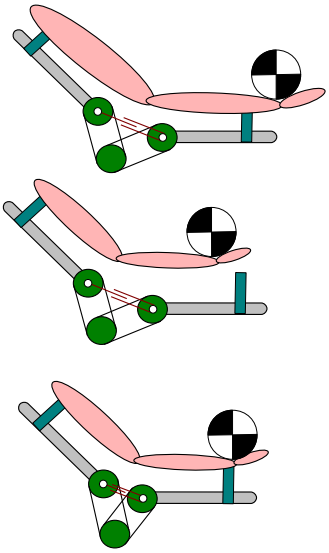

(d) Concept IV

FIGURE 2: *All concepts show two different sized users. The top image is the P95 user and the bottom the P05 user. The middle image shows the error between the concept setup for the P95 user and a P05 user with exception of (c). (a) This concept uses a rotation of the whole system to adapt to its user. (b) In this concept a lockable double hinge is used to adjust the length of the lower arm. (c) The system is designed to fit the smallest and largest person without adjustment. (d) Based on the system designed by Stienen et al. [3] including a linear guide.*

justment a bulky hinge is required. Finally concept III (Fig. 2c) has no adjustment. If there is no adjustment, the resulting system is simple and robust. The main drawback is that the shape is non-optimal for different sized users.

3.2 Evaluation

This section addresses the evaluation of the concepts shown in Fig. 2.

The breakdown into basic elements is used to evaluate the concepts. The elements are compared on their relative complexity to each other. In addition, the number of elements per concept are counted. Finally the systems are tested in dynamic software package to assess if the systems can transmit load forces and adapt to different users.

Concept I is shown in Fig. 2a and uses the rotation of multiple elements to adapt to it is user. A drawback is that the system must adjust it self during motion.

Concept II (Fig. 2b) depends on a rotating body to which the lower link is connected. The main drawback of this approach is that the rotating body must be locked to prevent movement. This implies a locking mechanism which may not be desired.

Concept III shown in Fig. 2c differs from the rest because it is designed to fit different user with out any adjustment. This concept uses a large spring to generate a force. A cable is used to control the elongation of the spring. The resulting force is used to counteract part the load forces. A drawback is that the spring can obstruct the user to move over objects like a bed. This results in a loss in range of motion. Moreover, the use of a large spring may result in a hazardous situation in case of malfunction.

Concept IV is shown in Fig. 2d and is based on the design made by Stienen et al. [3]. The limitation here is that the system can not counteract the reaction force in all positions. In addition, the force transmitted through cables limits the design of a compact system.

3.3 Final Concept

With the features of concepts I and III a final concept is designed. The following two features are used for this final concept. The use of relative movement between the exoskeleton and the user in concept I for adjustment. This working principle is the most promising feature to design a system which requires no active adjustment to the user. The second feature use is the rigid connection between the lower arm and the exoskeleton as in concept III. A degree of freedom analysis shows that a rigid connection is needed to transfer the load force to the environment. The corresponding design is shown in Fig. 3.

The final system lets the user's elbow move with respect to the system, which eliminates the need for alignment. The reaction forces are eliminated by rigidly connecting the lower arm to the exoskeleton. Detailed analysis is done in the section that follows. This concept has two key features.

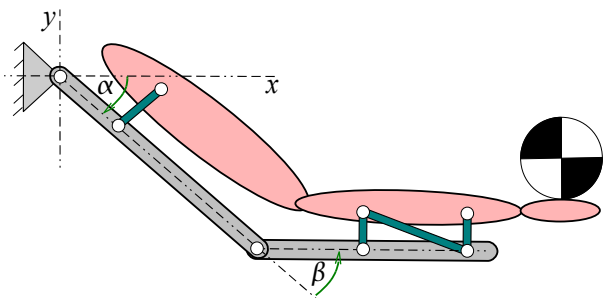

FIGURE 3: *The final concept which fulfills both design goals. The elbow and shoulder can move relative to the exoskeleton which eliminates the need for alignment. The rigid connection between the lower arm and the exoskeleton transfers all load forces to the environment.*

Rigid connection to the lower arm
Connecting the lower arm to the system makes it possible to transfer all load force to the environment.
Disconnected shoulder joint and one connection to the upper arm
This makes it possible to eliminate the reaction forces in the user's elbow and allows the elbow to move with respect to the system.

4 DETAILED DESIGN

The chosen concept in the previous section provides the basis for a detailed design. To this end the actuation of the system was not discussed. It is chosen to investigate the potential to use springs for gravity compensation. The design is shown in Fig. 4 with all relevant design parameters.

The introduction of an additional rigid element in the system results in a translational motion between link *JN* and *DH* that depends on β. This translation can be used to store the potential energy change by the mass due to the change of height. The connection between the lower arm and system can be placed arbitrary.

A spring is modeled for gravity compensation. The potential energy in the system is used to assist in the designing of the system. To calculate the potential energy, all kinematics are determined. Hence an analytical model is made that calculates all positions that correspond with input angles α and β.

4.1 Analytical Model

With the use of a software package an analytical model is created. The model is based on a kinematic chain algorithm which starts at the base connection *A*. Point *A* is chosen as start

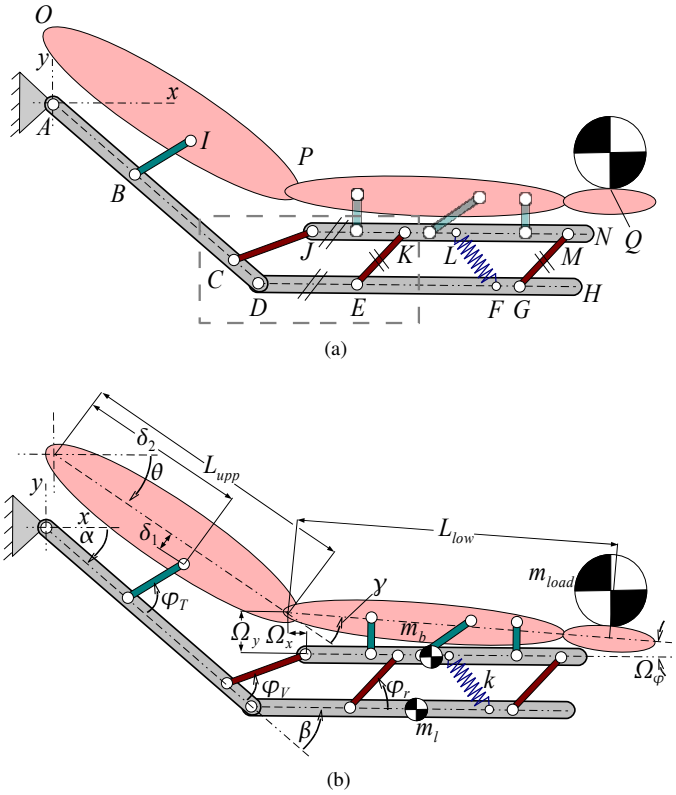

FIGURE 4: *Schematic representations of the end design. The masses m_l and m_b are located at the center of the corresponding bodys. (a) Connections points displayed. Link EK is parallel to GM. Link JN is parallel to DH. The dashed box indicated the points used for the four-bar calculation. (b) Ω_x, Ω_y and Ω_ϕ quantify the alignment error of the lower arm. δ_1 and δ_2 are used to position the connection to the upper arm. k is the spring stiffness.*

point because it is the base point, which does not depends on α and β. α and β are used as input for this model, since these are the angles the actuator acts upon.

The location of the joint *D* is depending on $|AD|$ and α.

$$D_x(\alpha) = |AD|\cos\alpha \tag{1}$$
$$D_y(\alpha) = |AD|\sin\alpha \tag{2}$$

Point *H* can be calculated with the location of point *D* and the additional relative position.

$$H_x(\alpha,\beta) = D_x + |DH|\cos(\alpha-\beta) \tag{3}$$
$$H_y(\alpha,\beta) = D_y + |DH|\sin(\alpha-\beta) \tag{4}$$

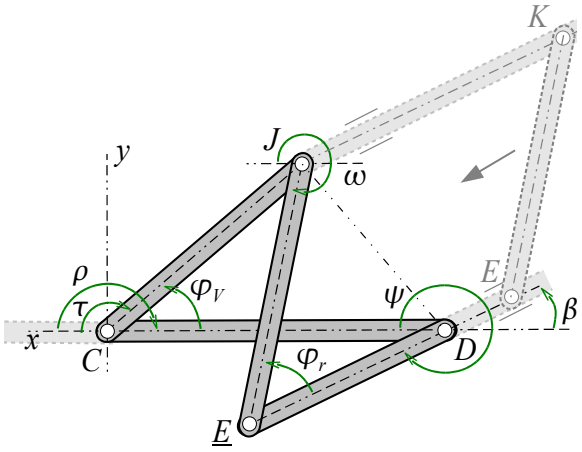

FIGURE 5: *Schematic representation of the model to calculate φ_r and φ_V. By moving link KE a virtual four-bar is made where $|D\underline{E}| = |DE| - |JK|$ and $|\underline{E}J| = |EK|$. The points C, D, E, K, J and angle β correspond with Fig. 4 indicated with a dashed box.*

Such a kinematic chain can be constructed for B, C, E, F and G in a similar way. To calculate the other points the dependence of φ_V, φ_r with respect to β is expressed.

A five-bar mechanism is defined by the following points C, D, E, K and J. The dashed box in Fig. 4a indicates the five-bar mechanism. Figure 5 shows the five-bar mechanism in more detail.

Calculating a five-bar mechanism is difficult, because there are multiple configurations possible with the same input angle. However link DE and link JK are parallel. This is due to the parallelogram made by points E, G, M and K. Link EK can be placed arbitrary if the link is kept parallel to link GM. This parallelogram property is used to move link EK untill K coincides with J, see Fig. 5. This movement results in a four-bar mechanism CD, $D\underline{E}$, $\underline{E}J$ and JC.

The four-bar mechanism is calculated with the use of the 'Freudenstein Equation' [14]. This equation is used to numerically calculate the two outputs (τ_1,τ_2) that correspond to the input angle (ψ). On account of the fact that a four-bar mechanism will always have two possible configurations for a given input angle.

The 'Freudenstein Equation' is based on the principle of a closed vector loop notation.

$$\vec{CD} + D\vec{\underline{E}} = \vec{CJ} + J\vec{\underline{E}} \tag{5}$$

The closed vector loop is divided into two components.

$$x: \quad |CD|\cos\rho + |D\underline{E}|\cos\psi = |CJ|\cos\tau + |J\underline{E}|\cos\omega \tag{6}$$
$$y: \quad |CD|\sin\rho + |D\underline{E}|\sin\psi = |CJ|\sin\tau + |J\underline{E}|\sin\omega \tag{7}$$

The reference frame is chosen equal to direction of vector $\vec{CD}$ which results in $\rho = \pi$. Furthermore, with the use of the 'Pythagorean formula' $(\cos^2\omega + \sin^2\omega = 1)$ variable ω is eliminated. This results in the 'Freudenstein Equation'

$$R_1\cos\tau - R_2\cos\psi + R_3 = \cos(\tau - \psi) \tag{8}$$

where

$$R_1 = \frac{|CD|}{|D\underline{E}|} \tag{9}$$
$$R_2 = \frac{|CD|}{|CJ|} \tag{10}$$
$$R_3 = \frac{|CD|^2 + |CJ|^2 + |D\underline{E}|^2 - |J\underline{E}|^2}{2|CJ||D\underline{E}|} \tag{11}$$
$$\psi = 2\pi - \beta. \tag{12}$$

With the use of the tangent half-angle formulas Eq. 13 the 'Freudenstein Equation' is rewritten to a quadratic formula.

$$z = \tan\frac{\tau}{2}, \quad \cos\tau = \frac{1-z^2}{1+z^2}, \quad \sin\tau = \frac{2z}{1+z^2} \tag{13}$$

τ is replaced with z according to the tangent half-angle formula.

$$R_1\frac{1-z^2}{1+z^2} - R_2\cos\psi + R_3 = \cos\psi\frac{1-z^2}{1+z^2} + \sin\psi\frac{2z}{1+z^2} \tag{14}$$

Equation 14 is rewritten to a standard quadratic notation

$$az^2 + bz + c = 0 \tag{15}$$

where

$$a = (R_1+1)\cos\psi + R_3 - R_2 \tag{16}$$
$$b = -2\sin\psi \tag{17}$$
$$c = (R_1-1)\cos\psi + R_2 + R_3. \tag{18}$$

The output τ is used to express the two angles φ_V and φ_r.

$$\varphi_r(\beta) = \arccos \frac{|\underline{JE}|^2 + |CD|^2 - |\underline{JE}|^2}{2|\underline{JE}||CD|} \tag{19}$$

$$\varphi_V(\beta) = \pi - \tau \tag{20}$$

The quadratic formula results in two solutions for the given four-bar mechanism. So for every β there are two corresponding φ_V and φ_r.

This model is used to calculate every position illustrated in Fig. 4a. This in return is used to determine if the system can adapt to its user. Additionally the mechanical potential energy in the system is evaluated in section 4.4.

4.2 Kinematics

The first goal is to design an exoskeleton that fits all users. With the use of the analytical model, three properties are evaluated.

- Adapting to the P05-P95 norm.
- Range of motion.
- Relation between the system (α,β) and user (θ,γ) angles.

The relation between the user angles and the system is important for the actuation of the system.

To check the three properties, a parameter set is chosen and is listed in Tab. 3. Figure 6 shows four plots of the analytical model.

Figure 6a and 6b shows the P05 size user. The chosen parameter set and design is capable to fit the P05 user. Figure 6c and 6d shows the P95 size user. With the same dimensions, the P95 user fits the exoskeleton. Hence, the exoskeleton can adapt to the P05-P95 norm.

The requirements state that the elbow must have a range of motion $[0 : \frac{\pi}{2}]$. In Fig. 6a and 6c the $\gamma = \frac{\pi}{2}$ position is shown. Figure 6b and 6d show the extended position $\gamma = 0$. This indicates that the range of motion for γ is reached. The range of motion for the shoulder is closely related to α. It can be concluded that this design does not limit the range of motion of the shoulder, so both requirements are met.

The difference between the system angles for the same user angles is clearly visible in Fig. 6b and 6d. Therefore it is concluded that the relation between θ, γ and α, β depends on the size of the user.

It is found that the design fulfills the requirements for a wide range of design parameters. There are a number of selection criteria that can be used to fulfill the soft requirements.

- Movement of the shoulder (O) with respect to the base (A).
- Movement of the elbow (P) with respect to the exoskeleton hinge (D).
- Design space under the lower arm.

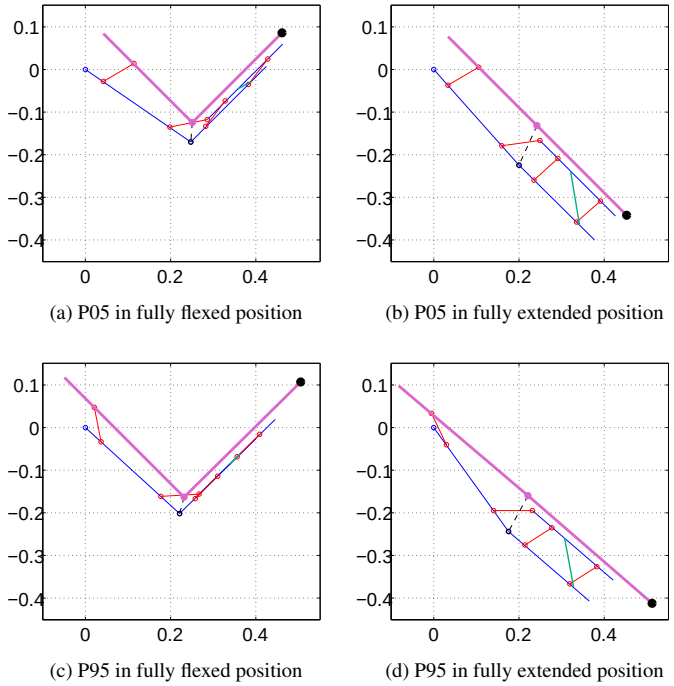

(a) P05 in fully flexed position

(b) P05 in fully extended position

(c) P95 in fully flexed position

(d) P95 in fully extended position

FIGURE 6: *Plots of the system based on the analytical model. All values are in meters. The base point is located at* $(0,0)$. *The pink lines indicate the user. The blue and red lines shows the exoskeleton. The green line shows the spring inside the exoskeleton. The black dot indicates the load.*

- Range of β with respect to the required range of γ.
- Range of α with respect to the required range of θ.

A demonstrator is constructed to verify the results of the analytic model. Section 5 will address the kinematic demonstrator in more detail.

Optimization is used to fulfill the soft requirements. It is chosen to focus on the spring gravity compensation of the system. This is discussed in Section 6.

4.3 Force Analysis

The second design goal is to reduce the reaction force in the human joint. Figure 7 displays an exploded view of the exoskeleton with the force directions. The reaction force F_r must be lower then the specified 115 [N].

It is proven that the system can have equilibrium without forces and moments in points O and P. The moments M_β and M_α are introduced to define the moments that need to be delivered by actuators. The spring is excluded, since it is not needed for an equilibrium.

The force and moment equilibria for each element are eval-

TABLE 3: *Parameters of analytical model and the demonstrator*

Parameter	Quantity	Unit
$\|AD\|$	0.3	m
$\|AB\|$	0.049	m
$\|BI\|$	0.083	m
$\|CD\|$	0.06	m
$\|CJ\|$	0.09	m
$\|DH\|$	0.25	m
$\|DE\|$	0.05	m
$\|EF\|$	0.15	m
$\|EK\|$	0.075	m
$\|JK\|$	0.06	m
$\|JN\|$	0.25	m

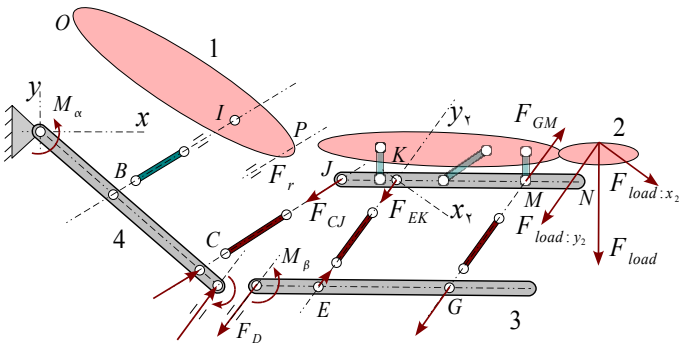

FIGURE 7: *Free body diagram of the exoskeleton. The spring is excluded. There are 4 main bodies numbered from 1 to 4 and 4 links. Body is 1 is the upper arm of the user. Body 2 is the lower arm of the user and link JN of the exoskeleton. Body 3 is the lower part of the exoskeleton and body 4 is the upper part of the exoskeleton. The four links are BI, CJ, EK, and GM.*

uated. In the 2D plane there are three equilibrium equations that need to be fulfilled.

$$\sum F_{x^*} = 0, \quad \sum F_{y^*} = 0, \quad \sum M = 0 \tag{21}$$

Where x^* and y^* direction can be chosen per element if y^* is perpendicular to x^*.

Selecting element BI with y^* is the longitudinal direction. A link connected with two joints can only achieve equilibrium in the y^* direction, if the connected joints do not apply a moment. A force in another direction or a moment does not result in equilibrium. Therefore all links with two joint connections have a force direction in there longitudinal direction as shown in Fig. 7.

The force and moment equilibria of body 1are evaluated. The direction of the force in link BI is equal to its direction. No force is present in point O as stated before. To achieve the two force equilibria, F_r must be in the same direction as the link BI. However, no moment equilibrium can be reached if $F_r \neq 0$.

From the previous statement it follows that $F_r = 0$. There are three forces acting on body 2. The directions of the corresponding forces are known. Setting y^* in the longitudinal direction of the links EK and GM results in the local frame of reference x_2, y_2. Dividing the load force F_{load} into the x_2 and y_2 components will result in F_{CJ} as the following equations state.

$$\vec{F_{load:x_2}} \cdot \vec{F_{EK}} = 0 \tag{22}$$

$$\vec{F_{load:x_2}} \cdot \vec{F_{GM}} = 0 \tag{23}$$

$$\vec{F_{load:x_2}} \cdot \vec{F_{CJ}} \neq 0 \tag{24}$$

Using the moment equilibrium and following the force equilibrium in the y_2 direction leads to F_{EK} and F_{GM}.

There are three forces acting on body 3. The force F_D must be in the same direction as F_{EK} and F_{GM}. M_β must be applied for moment equilibrium.

Finally body 4 is evaluated. Body 4 transfers the forces F_D, F_{CJ} to the environment. M_α is used for moment equilibrium.

The system can be in equilibrium while preventing a reaction force in the elbow. There is one condition that needs to be fulfilled.

$$\vec{CJ} \times \vec{EK} \neq 0 \tag{25}$$

If this condition is not satisfied no force equilibrium of body 2 can be reached. This must be considered during design.

4.4 Energy Analysis

Using the kinematic model, the potential energy in the system is assessed. If the potential energy is constant over the range of motion, the system can be moved almost effortless [15]. A helical spring inside the exoskeleton is proposed to keep the potential energy fluctuation small. A helical extension spring is chosen because it is widely available and has a high energy storage density [16].

The gravitational potential energy of a mass E_m only depends on the relative height with respect to a chosen reference [17]. In addition, elastic potential energy of a helical extension

spring E_k depends on the spring stiffness k and the elongation of the spring u.

$$E_m(\alpha,\beta) = mgh \tag{26}$$
$$E_k(\beta) = {}^1\!/_2 ku^2 \tag{27}$$

where g is the gravity field, m the mass and h the relative height.

The total potential energy in the system is the sum of energies

$$E_p = \sum_{i=1}^{n} m_i g h_i + \sum_{j=1}^{m} {}^1\!/_2 k_j u_j^2 \tag{28}$$

where n is the amount of mass bodies in the system and m the number of springs. Figure 8 shows the mechanical potential energy in the system.

Using the relationship between the potential energy and the moment, the resulting moments are calculated [18].

$$M_\theta = -\frac{\partial E_p}{\partial \theta} \tag{29}$$

The combination of the potential energy and the moments give a prediction of the system's behavior. This can be used to design an actuator for the system.

5 DEMONSTRATOR

A demonstrator is constructed to check if the system can passively adapt to its user. Furthermore, the demonstrator is used to verify the mathematical model. Table 3 lists the design parameters used for the demonstrator. The system is made out of wood, aluminum and steel. For the connection to the user Velcro is used.

The demonstrator consists out of two segments. These two segments are connected in the out of plane direction. The distance between the segments is 0.12 [m].

5.1 Evaluation

Two wooden mock-ups which have the maximum and minimum dimensions as listed in Tab 1 where made. The mock-ups represent the human bodies made by OP and PQ shown in Fig. 4. These mock-ups were used to verify if the kinematics allow passive alignment. Furthermore the mock-ups are used to test the range of motion in the 2D plane. Figure 9 shows the mock-ups in the demonstrator.

With the chosen design parameters the exoskeleton does not exceed the 0.12 [m] design space.

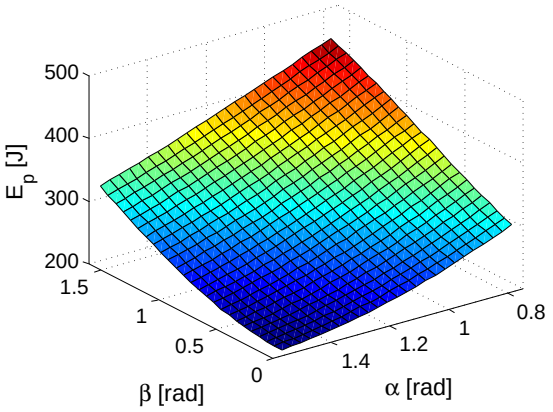

FIGURE 8: *The mechanical potential energy in the system calculated with the analytical model. α and β are the angles of the exoskeleton. The P05 sized user is modeled in this plot. The base point A_y, as shown in Fig. 4 is 1 meter from the reference plane. The load is chosen as 40 kilogram. Furthermore, the mass of the exoskeleton is included and are estimated at $m_b = 1,5$ kilogram and $m_l = 2$ kilogram.*

Both the P05 and P95 mock-up fit in the demonstrator without any adjustment. The requirement to adapt to its user is fulfilled.

The photos in Fig. 9 show that the elbow does not reach the required $\frac{\pi}{2}$. This is because the elements which make up the demonstrator are in the same plane and collide. So the range of motion of the demonstrator is too limited to proved the required range of motion for the user.

6 Optimization

The analytical model provides a basis to numerically optimize the design parameters. The goal is to minimize the potential energy fluctuation in the system, since this will lead to an energy efficient system. In addition, a constant moment is preferred since this leads to predictable behavior for the user.

The spring in the proposed design only affects M_β. It is chosen that the optimization focuses on β and α is set on $\frac{\pi}{4}$. A design vector $\mathbf{s}$ is chosen.

$$\mathbf{s} = [|CJ|, k, l_{k0}, |JK|, |DF|] \tag{30}$$

A genetic algorithm (GA) is used to find sets of parameters within design vector $\mathbf{s}$ that give a desired outcome. A GA tests a large number of parameter sets and returns the parameter sets

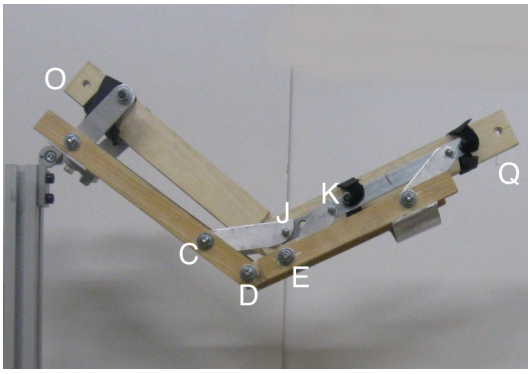

(a) P05 in fully flexed position

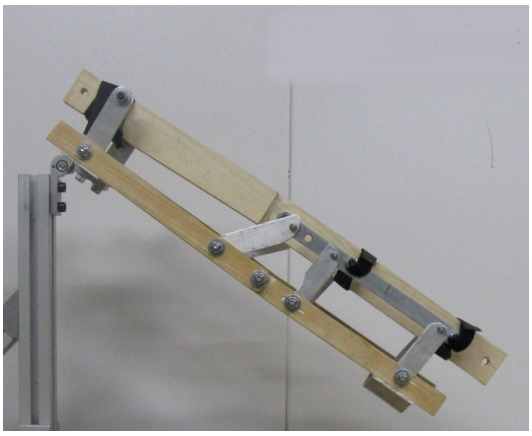

(b) P05 in fully extended position

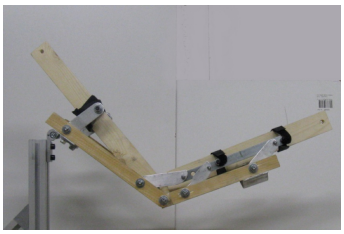

(c) P95 in fully flexed position

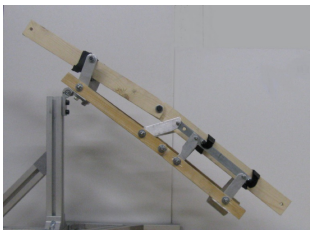

(d) P95 in fully extended position

FIGURE 9: *Photos of the demonstrator with two wooden mock-ups. The mock-up represents the user indicated by points O,P and Q.*

which is closest to the desired goal. The benefit of GA is that it can cope with complex fitness functions. A drawback is that GA can give a local minimum as outcome. As a result it is unknown if the outcome is the absolute optimum.

A fitness function is formulated to achieve the optimization goal. Equation 31 shows the fitness function.

$$\min_{\mathbf{s}} \left(\lambda_1 \cdot f_{M_\beta}(\mathbf{s}) + \lambda_2 \cdot f_{E_p}(\mathbf{s})\right) \tag{31}$$

where

$$f_{M_\beta}(\mathbf{s}) = \int_0^{\frac{\pi}{2}} \left[M_\beta(\mathbf{s},\beta) - \bar{M}_\beta(\mathbf{s})\right]^2 d\beta \tag{32}$$

$$f_{E_p}(\mathbf{s}) = \int_0^{\frac{\pi}{2}} \left[E_p(\mathbf{s},\beta) - \bar{E}_p(\mathbf{s})\right]^2 d\beta \tag{33}$$

The function is constructed out of two sub functions. Sub function f_{M_β} relates to the moment fluctuation. The sub function f_{E_p} relates to the potential energy change in the system. $\bar{M}_\beta$ and $\bar{E}_p$ are the mean values of the corresponding moment and potential energy.

Minimizing the sub function f_{E_p} results in near constant potential energy, which in result leads to an energy efficient system. However, a minimal value of f_{E_p} can still contain large moment fluctuations. Sub function f_{M_β} effects the fluctuation of the moment. It is preferred to have a constant moment since this leads to predictable system behavior for the user. Two weight factor λ_1, λ_2 are to used combine these two sub functions.

There are two evaluation criteria used to indicate the performance of the gravity compensation. Both evaluation criteria are based on the moment M_{opti}. M_{opti} is the moment around β with the optimized gravity compensation. In the evaluation criteria $M_{\beta,0}$ indicated the moment around β without gravity compensation.

$$\Delta_M = 100 - \frac{\max|M_{opti}| - \min|M_{opti}|}{\max|M_{\beta,0}| - min|M_{\beta,0}|} \cdot 100[\%] \tag{34}$$

$$\Delta_E = 100 - \frac{\max|M_{opti}|}{\max|M_{\beta,0}|} \cdot 100[\%] \tag{35}$$

Equation 35 indicates the reduction of the maximum slope in the energy change which is the moment. If the potential energy is constant $\Delta_E = 100\,\%$. Δ_M shows the amount of moment fluctuation reducing achieved. If the resulting moment is constant, $\Delta_M = 100\,\%$.

The potential energy in the system depends on the masses in the system listed in Tab. 4. The begin design parameters are chosen the same as the demonstrator listed in Tab. 3.

It is chosen to select the weight factor in so that the influence of f_{E_p} and f_{M_β} are near equal. The moment fluctuates around 30 $[Nm]$ and the potential energy varies around 130 $[J]$ before optimization. The weight factor are set at $\lambda_1 = 4$ and $\lambda_2 = 1$.

Figure 10 shows the moments with and without gravity compensation. The two reductions are $\Delta_E = 98.8\%$ and $\Delta_M = 96.8\%$. The corresponding parameter values from the optimization are listed in Tab. 5. Figure 11 shows the system with the optimized parameters.

TABLE 4: *Masses used for the optimization. The load m_{load} is based on a patient of 80 kilogram. For one arm the load is selected 40 kilogram. The mass of the exoskeleton are estimated*

Parameter	Quantity	Unit
m_l	2	kg
m_b	1.5	kg
m_{load}	40	kg

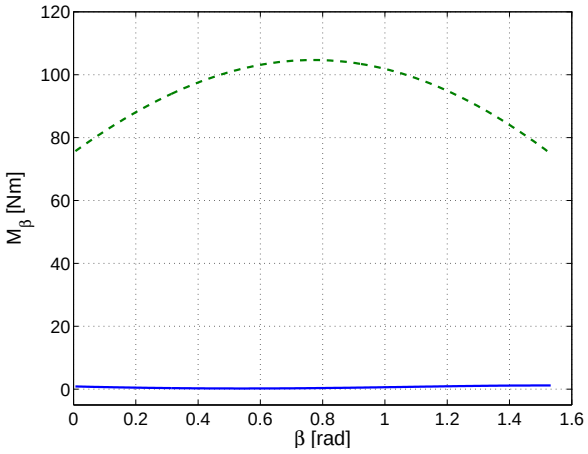

FIGURE 10: *Moment around β with the optimized gravity compensation. The masses are listed in Tab. 4. For this plot $\alpha = \frac{\pi}{4}$. The dashed line is the moment without gravity compensation $M_{\beta,0}$. The solid line is the moment with the optimized gravity compensation M_{opti}.*

TABLE 5: *Parameters output from the optimization.*

Parameter	Quantity	Unit
$\|CJ\|$	0.0562	m
k	8531	$\frac{N}{m}$
L_{k0}	0.0143	m
$\|JK\|$	0.0502	m
$\|DF\|$	0.1828	m

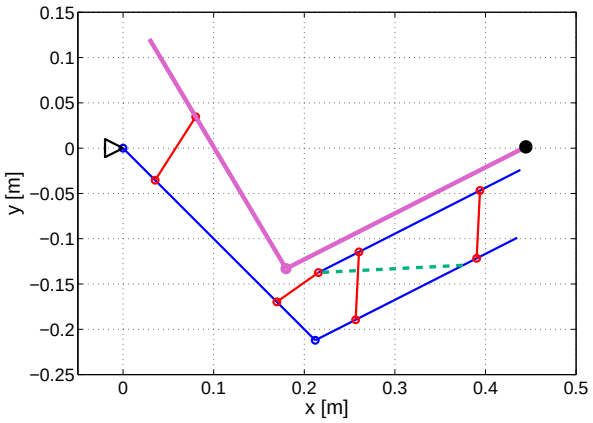

FIGURE 11: *Plot of the design with the optimized parameters. The green dashed line indicates the spring within the system. The pink lines indicate the P05 sized user. The blue and red lines shows the exoskeleton. The exoskeleton is connected to the environment at the base point* $(0,0)$.

7 DISCUSSION

This section addresses a number of topics of the design process. The design, the connection between the user and the system, the optimization of the system and two DoF gravity compensation are discussed. Finally recommendations for future research and development are made.

7.1 Design

The current design has a connection hinge between the upper arm and the exoskeleton. The force analysis showed that there is no force in the connecting link *BI*. The link *BI* is only used to make a closed kinetic chain between the user and the exoskeleton. If the user does not follow the movement of the exoskeleton a reaction force in the shoulder, elbow and the connection link *BI* will arise.

Removing this link results in an under constrained system. A benefit of removing the connecting link *BI* is that the shoulder can move freely. In addition, the chance of reaction forces in the elbow is reduced. The angles of the user and the exoskeleton do not depend on the user angles. This difference can be a drawback for actuation and gravity compensation.

To design this exoskeleton within a 3D environment brings some difficulties. The gravity compensation is design in the assumption that the exoskeleton is alway underneath the users arm. If the exoskeleton is not in line with the gravity field the exoskeleton will not work. To prevent the exoskeleton to move out of line with the gravity field two solutions are proposed. One

solution is to limit the range of motion of the user so the exoskeleton will stay upright. A second solution is to design a hinge mechanism that allow the exoskeleton to be in the line of the gravity field in depended of the position.

When the exoskeleton will be used, the loads lifted will vary. Adjusting the gravity compensation is desired to maintain an energy efficient exoskeleton. This can be achieved by changing the relative angle of the springs which results in a different energy curve. Another approach is to use multiple springs which then can be activated or deactivated. This will change the effective stiffness of the system.

This project focuses on a lifting case. Increasing the range of motion this design can assist the care providers in other demanding tasks. In addition, this design can be used in various other application fields which are demanding on the human body.

This exoskeleton design is the first elastic gravity compensated design. Using springs an energy efficiency of over 90% is reached. The unique combination of springs and fit shape leads to a new field of exoskeletons.

7.2 Connection between user and system

In this paper no steps were taken into designing the connection between the user and the system. In the proposed system the force of the load is applied to the user. Transferring the force from the user to the system must be done through the skin. A risk is present that the forces will damage the skin. In particular shear forces can cause damage to the skin [19]. There is a relation between the duration and the amplitude of the force acting on the skin

$$\alpha P \cdot \beta t = c \tag{36}$$

where P is the amplitude of the force in $^{N}/_{m^2}$, t the duration of the force in seconds and α, β, c are experimental constants. The value of α, β and c vary by experiment [19].

In the presented lifting case the duration of the load (t) is short which in result allows a greater load (P), nevertheless the skin is a limiting factor. When using the system for high loads it is preferred to transfer the load force directly to the system. This results in an end-point manipulator, which has a different design space then an exoskeleton.

7.3 Optimization

The optimization used in this paper focusses on the potential energy in the system for gravity compensation. There are more soft requirements like; a compact, light, cheap and simple system with minimal movement restrictions. If these soft requirements are quantified, they can be included in the fitness function. In addition, selecting another design vector can be used to fulfill the soft requirements.

The optimization in this paper is used to show gravity compensation in the proposed design. To test the gravity compensation with a demonstrator a number of issues must be solved. It is hard to find a spring with the exact properties given by the optimization. To overcome this issue the design vector can be changed to optimize around an existing spring. Since the spring is located in a parallelogram the effective stiffness can be achieved by multiply springs. Furthermore, dimensional tolerance introduce variations to a demonstrator. To determine the allowed tolerance, the robustness to variations of the design parameters must be analyzed.

Now a standard helical tension spring is modeled. Using other types of springs, a different energy curve can be reached. composite springs can be constructed in various shapes with different energy curves. Furthermore, composite springs can reach a higher energy per mass storage. Designing the exoskeleton together with a composite spring can lead to a lighter, compact and better preforming design.

7.4 Two degrees of freedom

The spring in the current exoskeleton design only influences one degree of freedom. An exoskeleton that has gravity compensation for both degrees of freedom needs to overcome two difficulties. The upper part of the exoskeleton is not balanced and the gravity compensation of the lower part depends on angle α.

There are a number of ways to balance the upper part. One solution is by repeating the working principle of the lower part to the upper part of the exoskeleton. For the lower arm the gravitation compensation needs to change according to α. A solution is to change the length $|CD|$ relative to α. The influence of $|CD|$ to the gravity compensation is sufficient to maintain a good moment reduction.

7.5 Recommendations

To achieve a light compact system with good gravity compensation properties it is recommended to investigate the use of composite springs. Further research must indicate if the ability to combine the spring and the rigid elements together, can lead to a compliant mechanism. Compliant mechanisms have a number of benefit over conventional mechanisms [20].

To use this exoskeleton design in other application fields, further research is needed on the requirements bases on other applications fields. For example, a car mechanic can use this exoskeleton to lift heavy car parts over his head while working underneath the car. This sets different requirements to the exoskeleton.

8 CONCLUSION

This project had the goal to design a mechanical system for the lower arm, which should fulfill two design goals. The first goal was that the system fits every user without active adjustment. The second goal was to reduce the reaction forces in the user. Both goals have been met. In addition, a start was made for gravity compensation using springs.

- A kinematic design has been proposed which easily fits the stated range of users.
- The kinematic design removes reaction forces from the body.
- A demonstrator was built and it was shown that it fits the P05-P95 range of users.
- The demonstrator constructed did not achieve the required range of motion of the elbow joint.
- Optimization showed that gravity compensation by use of a spring is feasible.

ACKNOWLEDGMENT

The authors wish to thank the InteSpring B.V. team which provided a nice and educational environment. In addition thanks goes out to the Agentschap NL. Point-One program for their financial support for this project.

REFERENCES

[1] Blokstra, A., C.A., Baan, H.C., Boshuizen, T.L., Feenstra, R.T., Hoogenveen, H.S.J., Picavet, H.A., Smit, A.H., Wijga, W.M.M., Verschuren, *Vergrijzing en toekomstige ziektelast. Prognose chronische ziektenprevalentie 20052025.* , RIVM research report, july 2007.

[2] Butter, M., Rensma, A., van Boxsel, J., Kalisingh, S., Schoone, M., Leis, M., Gelderblom, G.J., Cremers, G., de Wilt, M., Kortekaas, W., Thielmann, A., Cuhls, K., Sachinopoulou. A., Korhonen, I., *Robotics for Healthcare*, Research report ordered by European Commission, DG Information Society, October 2008

[3] Stienen, A.H.A., Hekman, E.E.G., van der Helm, F.C.T., Prange, G.B., Jannink, M.J.A., Aalsma, A.M.M., van der Kooij, H., *Dampace: Design of an Exoskeleton for Force-Coordination Training in Upper-Extremity Rehabilitation*, ASME, Journal Mechanical Devices, Vol. 3, September 2009

[4] Stienen, A.H.A., *Development of Novel Devices for Upper-Extremity Rehabilitation*, Ph.D. Thesis, Dep. of Mechanical Engineering, University of Twente, The Netherlands, 2009.

[5] Koyama, T., Yamano, I., Takemure, K., Maeno, T., *Multi-Fingered Exoskeleton Haptic Device using Passive Force Feedback for Dexterous Teleoperation*, IEEE, International Conference on Intelligent Robots and Systems, Lausanne, Switzerland, October 2002

[6] Zoss, A.H., Kazerooni, H., Chu, A., *On the Mechanical Design of the Berkeley Lower Extremity Exoskeleton*, IEEE, International Conference on Intelligent Robots and Systems, Edmonton, Canada, 2005

[7] Schiele, A., van der Helm, F.C.T., *Kinematic Design to Improve Ergonomics in Human Machine Interaction*, IEEE Transactions on Neural Systems and Rehabilitation Engineering, Vol. 14, No. 4, December 2006

[8] Schiele, A., *Fundamentals of Ergonomic Exoskeleton Robots*, Ph.D. Thesis, Dep. of Mechanical Engineering, Delft University of technology , The Netherlands, 2008.

[9] Stienen, A.H.A., Hekman, E.E.G., van der Helm, F.C.T., van der Kooij, H., *Self-Aligning Exoskeleton Axes Through Decoupling of Joint Rotations and Translations*, IEEE Transactions on Robotics, Vol. 25, No. 3, June 2009

[10] Stienen, A.H.A., Hekman, E.E.G., van der Kooij, H., *Orthesis*, World Intellectual Property Organization (WO 2008/043508 A1), 2008.

[11] Matek, W., Muhs, D., Wittel, H., Becker, M., *Roloff/Matek Machine-onderdelen*, Academic Service, Schoonhoven, The Netherlands, Second Edition, 1996.

[12] Waters, T.R., Putz-Anderson, V., Grag, A., *Applications Manual for the Revised Niosh Lifting Equation*, U.S. Department of health and human services , Ohio, The United States, January 1994.

[13] Dined, *http://dined.io.tudelft.nl/dined/nl*, Visited, June 1 2010.

[14] A., Ghosal, *The Freudenstein Equation: Desing of Four-Link Mechanisms*, Resonance, Vol. 15, No. 8, pp. 699-710, Bangalore, India, August 2010.

[15] Herder, J.L., *Conception of balanced spring mechanisms*, Dep. of Mechanical Engineering, Delft University of Technology, The Netherlands, 1998.

[16] van Osch, F.J.C., Herder, J.L., *Mechanical spring design guide based on absorbed potential energy*, Literature survey, Dep. of Mechanical Engineering, Delft University of technology , The Netherlands, June 2010.

[17] Meriam, J.L., Kraige, L.G., *Engineering Mechanics: Statics*, John Wiley & sons, INC., New York, US, Third Edition, 1993.

[18] Meriam, J.L., Kraige, L.G., *Engineering Mechanics: Dynamics*, John Wiley & sons, INC., New York, US, Third Edition, 1993.

[19] Danz, M.H., *Belastbaarheid van de menselijke huid op druk- en schruifkracht*, MSc thesis, Delft University of technology , The Netherlands, June 1985.

[20] Howell, L.L., *Compliant Mechanisms*, John Wiley and Sons Inc., New York, US, 2001.

Contents

Appendix A

Concepts

A.1 Basic elements

Number: 1
Name: Link
Function: Make static connection between multiple points.
Graphical Representation:

Number: 2
Name: Joint
Function: Creates point of rotation between multiple body's.
Graphical Representation:

Number: 3
Name: Linear Guide
Function: Translating DoF between to points.
Graphical Representation:

Number: 4
Name: Body Connection
Function: Connection between body segment and system.
Graphical Representation:

Number: 5
Name: Cable
Function: Transfers a pulling force between to points.
Flexible in all other directions.
Graphical Representation:

Number: 6
Name: Pully
Function: Guiding a cable.
Graphical Representation:

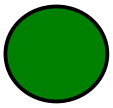

Number: 7
Name: Tread spindel
Function: Transfer rotation motion to linear motion.
Graphical Representation:

Number: 8
Name: Flex-Rigid
Function: Same as 1 (Link) but can change position between points.
Transform from rigid body to flexible body and vise versa.
Graphical Representation:

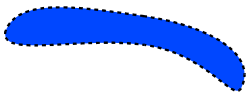

Number: 9
Name: Foam
Function: Make contact between two surfaces by elastic deformation.
Graphical Representation:

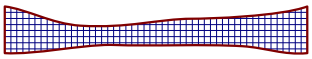

Number: 10
Name: Foam-solid
Function: Same as 9 but can become a solid body.
Graphical Representation:

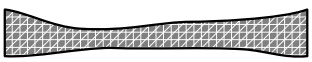

Number: 11
Name: Octoarm
Function: Make controllable curve (Paul Breedveld).

Graphical Representation:

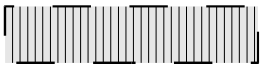

Number: 12
Name: Extension Spring
Function: Apply a force propositional to its elongation.
Graphical Representation:

Number: 13
Name: Torsion Spring
Function: Apply a force propositional to its rotation.
Graphical Representation:

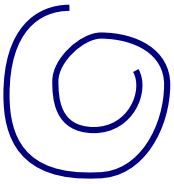

A.2 Concepts

The concepts which are evaluated.

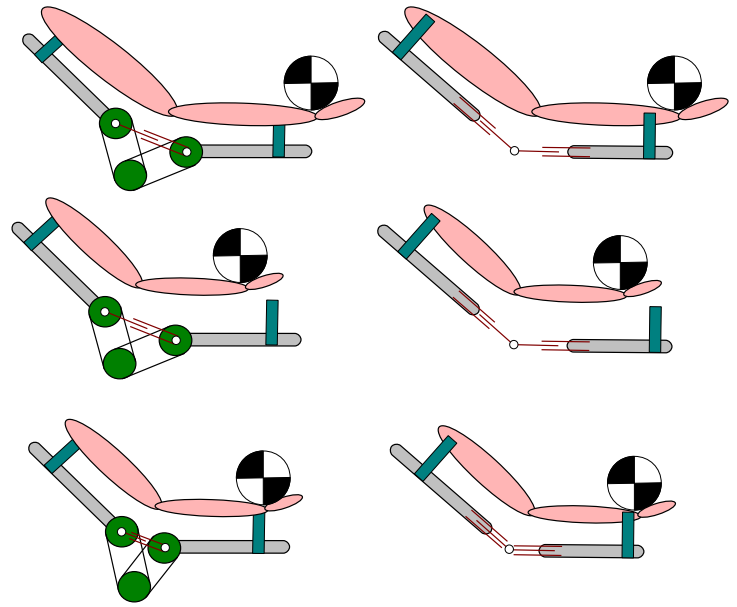

(a) Concept I *(b) Concept II*

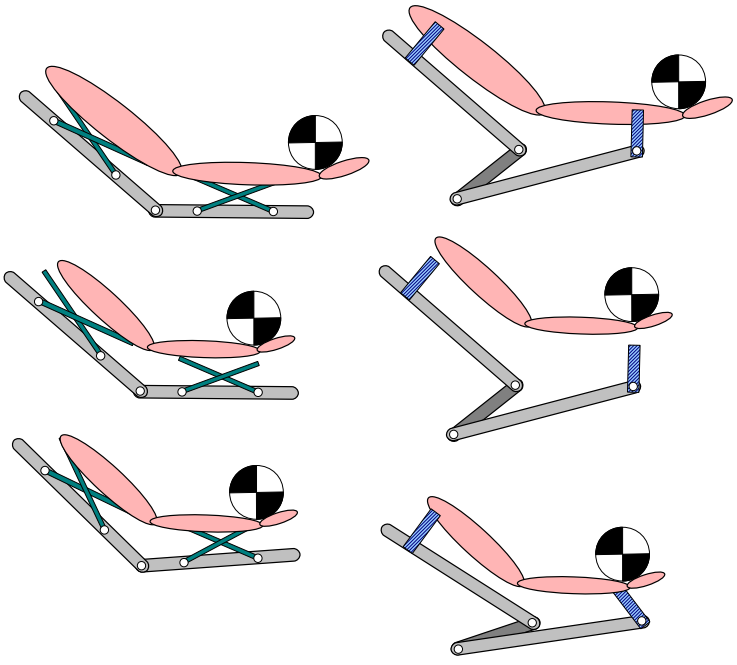

(c) Concept III *(d) Concept IV*

Figure A.1: Schematic representation of the first four concepts.

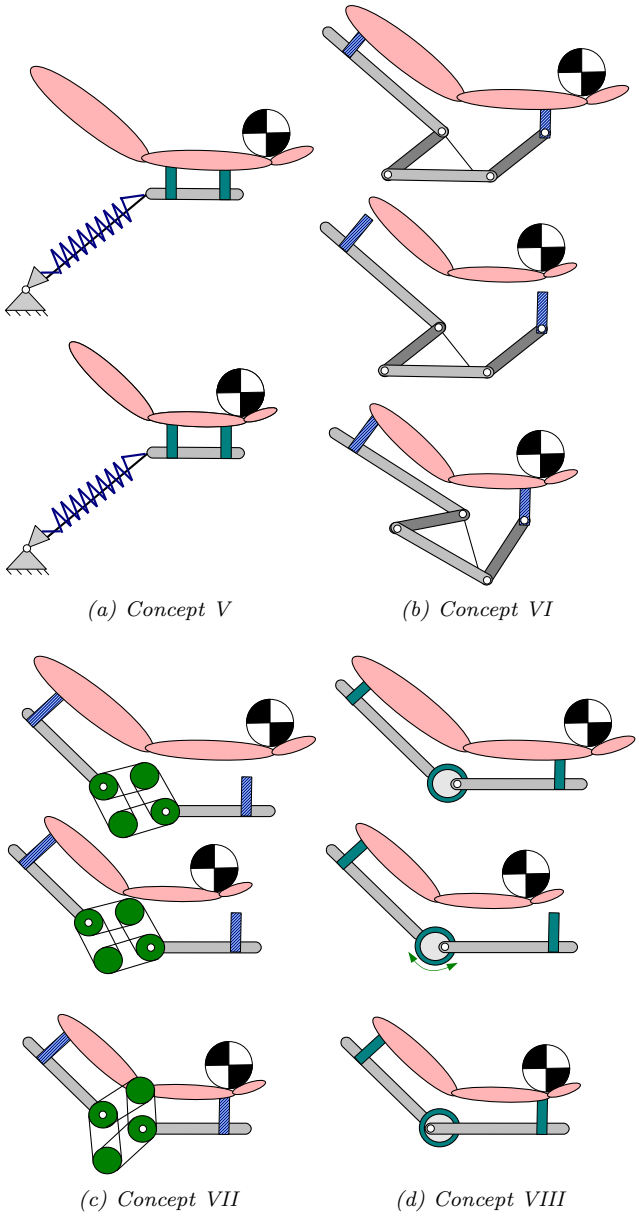

(a) Concept V *(b) Concept VI*

(c) Concept VII *(d) Concept VIII*

Figure A.2: Schematic representation of concepts V to VIII.

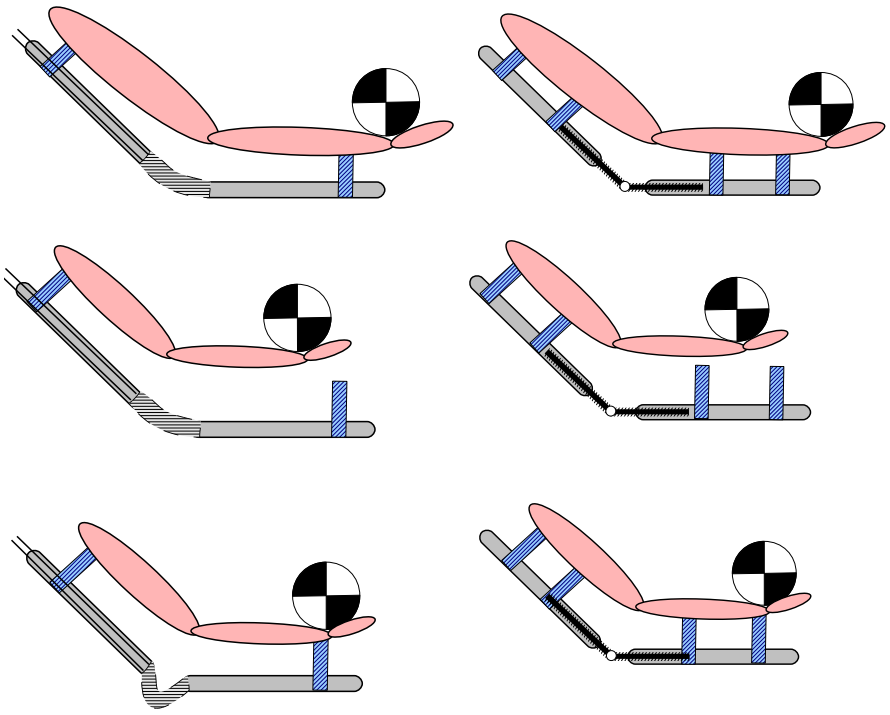

(a) Concept IX *(b) Concept X*

Figure A.3: Schematic representation of concepts IX to X.

A.3 Evaluation

In this section the evaluation of the concepts given in the previous section are discussed. First the number of basic elements is assessed and are listed in Tab. A.1.

Table A.1: Number of basic elements used in the concepts showed in Fig. A.1 - A.3.

Concept	I	II	III	IV	V	VI	VII	VIII	IX	X
Link	2	2	2	3	1	4	2	2	2	2
Joint	2	1	5	3	1	4	2	2		1
Linear Guide	1	2								
Body Connection	2	2	4	2	2	2	2	2	2	4
Cable	4				1	1	12		2	
Pulley	3						6			
Thread Spindel										2
Octoarm									2	
Extension spring					1					
Rigid body					1			2		
Total	14	7	11	8	7	11	24	8	7	9

For each basic element a weight function is assigned (Tab. A.2). The higher number are less preferred then lower numbers.

Table A.2: Weight values used for evaluation.

	Complex	Mass	Cost	Size
Link	1	4	4	3
Joint	1	1	5	1
Linear Guide	4	3	7	4
Body Connection	2	2	5	4
Cable	1	1	3	1
Pulley	2	3	4	3
Thread Spindel	3	6	7	4
Octoarm	7	4	20	4
Extension spring	2	5	6	5
Rigid body	2	4	7	3
Total Weight factor	1	1	1	2

Table A.3: Values form the valuation.

Concept	I	II	III	IV	V	VI	VII	VIII	IX	X
Amount of parts	14	7	11	8	7	11	24	8	7	9
Complex	22	15	15	10	11	13	24	12	15	17
Mass	31	21	21	19	19	25	36	22	18	29
Cost	59	37	53	37	35	49	64	42	44	47
Size	33	23	27	20	21	25	38	22	20	31

The best values are set on 1 the worst are 0. In this way a normalized grade is found. This is add up to find the best concept.

Table A.4: The normalized values for the given property.

Concept	I	II	III	IV	V	VI	VII	VIII	IX	X
Amount of parts	0.4	1.0	0.6	0.9	1.0	0.6	0.0	0.9	1.0	0.8
Complex	0.3	0.6	0.6	1.0	0.9	0.8	0.0	0.9	0.6	0.5
Mass	0.4	0.8	0.8	0.9	0.9	0.6	0.0	0.8	1.0	0.4
Cost	0.4	0.9	0.4	0.9	1.0	0.5	0.0	0.8	0.7	0.6
Size	0.8	1.7	1.2	2.0	1.9	1.4	0.0	1.8	2.0	0.8
Type	2.0	0.0	2.0	0.0	0.0	0.0	2.0	0.0	0.0	0.0
Total size	0.8	2.0	1.6	0.8	0.0	0.4	0.8	2.0	1.6	2.0
Total	5.1	**7.0**	**7.2**	**6.5**	5.7	4.0	2.8	**7.2**	**6.9**	5.1

There are five concepts with have a higher score then the rest. II, III, IV, VIII and IX.

Appendix B

Four-bar calculations

This appendix discusses the calculation on a four-bar mechanism in more detail then the paper. The 'Freudenstein Equation'[1] is used is these equations.
Starting a vector loop over the four-bar mechanism is constructed (Fig. B.1). The connection between a and b is the origin (A). The vector loop as follows

$$AB + BC = AD + DC \tag{B.1}$$

The above equation can be made for the x and y components. Link a is positioned in the negative x direction, therefore $\theta = \pi$

$$x: \quad b\cos\alpha + c\cos\varphi = a\underbrace{\cos\theta}_{=-1} + d\cos\beta \tag{B.2}$$

$$y: \quad b\sin\alpha + c\sin\varphi = a\underbrace{\sin\theta}_{=0} + d\sin\beta \tag{B.3}$$

Rewriting.

$$c\cos\varphi = -b\cos\alpha - a + d\cos\beta \tag{B.4}$$

$$c\sin\varphi = -b\sin\alpha + d\sin\beta \tag{B.5}$$

[1] A., Ghosal, *The Freudenstein Equation: Desing of Four-Link Mechanisms*, Resonance, Vol. 15, No. 8, pp. 699-710, Bangalore, India, August 2010.

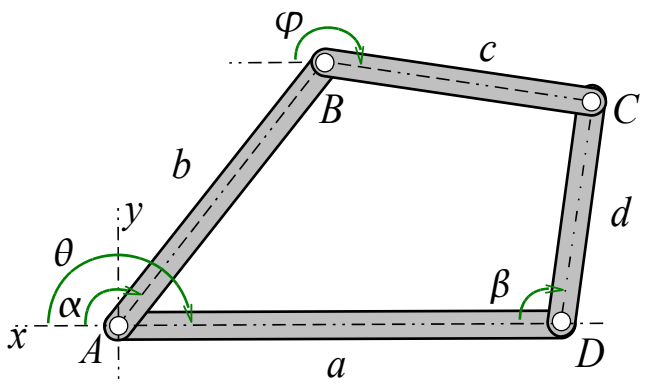

Figure B.1: Schematic four-bar used for the calculation.

Using the 'Pythagorean formula' $[\cos^2\varphi + \sin^2\varphi = 1]$ the variable φ is eliminated.

$$c^2\cos^2\varphi = [-b\cos\alpha - a + d\cos\beta]^2 \tag{B.6}$$
$$c^2\sin^2\varphi = [-b\sin\alpha + d\sin\beta]^2 \tag{B.7}$$

Combing the above equations Eq. B.6 and Eq. B.7 result in;

$$c^2\underbrace{(\cos^2\varphi + \sin^2\varphi)}_{=1} = [-b\cos\alpha - a + d\cos\beta]^2 + [-b\sin\alpha + d\sin\beta]^2 \tag{B.8}$$

Determining the two square expressions of the right hand terms in Eq. B.8.

$$\begin{aligned}[-b\cos\alpha - a + d\cos\beta]^2 =& b^2\cos^2\alpha + 2ab\cos\alpha - 2bd\cos\alpha\cos\beta + d^2\cos^2\beta \\ & - 2ad\cos\beta + a^2 \end{aligned} \tag{B.9}$$
$$[-b\sin\alpha + d\sin\beta]^2 = b^2\sin^2\alpha - 2bd\sin\alpha\sin\beta + d^2\sin^2\beta \tag{B.10}$$

Substituting equations B.9, B.10 into equation B.8.

$$\begin{aligned}c^2 =& b^2\underbrace{(\cos^2\alpha + \sin^2\alpha)}_{=1} + d^2\underbrace{(\cos^2\beta + \sin^2\beta)}_{=1} + 2ab\cos\alpha - 2ad\cos\beta \\ & - 2bd(\cos\alpha\cos\beta + \sin\alpha\sin\beta) + a^2 \end{aligned} \tag{B.11}$$

Having one equation with one output variable β the equation is written as the 'Freudenstein equation'

$$\frac{a^2 + b^2 - c^2 + d^2}{2bd} + \frac{a}{d}\cos\alpha - \frac{a}{b}\cos\beta = \underbrace{\cos\alpha\cos\beta + \sin\alpha\sin\beta}_{=\cos(\alpha-\beta)}$$
$$R_1\cos\alpha - R_2\cos\beta + R_3 = \cos(\alpha - \beta) \tag{B.12}$$

where

$$\begin{aligned}R_1 =& \frac{a}{d} \\ R_2 =& \frac{a}{b} \\ R_3 =& \frac{a^2 + b^2 - c^2 + d^2}{2bd}.\end{aligned}$$

Equation B.12 is the 'Freudenstein equation'. Using the half tangent rules (Eq. B.13) Eq. B.12 is rewritten to a exponential function.

$$x = \tan\frac{\beta}{2}, \quad \cos\beta = \frac{1 - x^2}{1 + x^2}, \quad \sin\beta = \frac{2x}{1 + x^2} \tag{B.13}$$

$$\begin{aligned}R_1\cos\alpha - R_2\cos\beta + R_3 =& \cos\alpha\cos\beta + \sin\alpha\sin\beta \\ R_1\cos\alpha - R_2\frac{1 - x^2}{1 + x^2} + R_3 =& \cos\alpha\frac{1 - x^2}{1 + x^2} + \sin\alpha\frac{2x}{1 + x^2} \\ R_1\cos\alpha + R_3 =& (\cos\alpha + R_2)\frac{1 - x^2}{1 + x^2} + \sin\alpha\frac{2x}{1 + x^2} \\ (R_1\cos\alpha + R_3)(1 + x^2) =& (\cos\alpha + R_2)(1 - x^2) + 2x\sin\alpha \\ R_1\cos\alpha + R_3 + (R_1\cos\phi + R_3)x^2 =& \cos\alpha + R_2 - (\cos\phi + R_2)x^2 + 2x\sin\alpha \end{aligned} \tag{B.14}$$

Equation B.14 is rewritten into a quadratic function.

$$[(R_1 + 1)\cos\alpha + R_3 + R_2]x^2 + [-2\sin\alpha]x + [(R_1 - 1)\cos\alpha + R_3 - R_2] = 0 \tag{B.15}$$

Using the half-tan rules equation B.12 is now expression in a simple quadratic expression

$$\bar{a}x^2 + \bar{b}x + \bar{c} = 0 \tag{B.16}$$

where

$$\begin{aligned}\bar{a} &= (R_1 + 1)\cos\alpha + R_3 + R_2 \\ \bar{b} &= -2\sin\alpha \\ \bar{c} &= (R_1 - 1)\cos\alpha + R_3 - R_2\end{aligned}$$

Using equations B.13 the new introduces variable x can be expressed in β

$$\beta_{1,2} = 2\arctan x_{1,2} \tag{B.17}$$

where

$$x_{1,2} = \frac{-\bar{b} \pm \sqrt{\bar{b}^2 - 4\bar{a}\bar{c}}}{2\bar{a}}. \tag{B.18}$$

Appendix C

Matlab code of the analytical model

There are a number of files used to make the analytical model.

- Runner.m
- Energy_cal.m
- Fourbar.m
- Fourbar2.m
- Plotter_runner.m

```
tic
%% Clearing the workspace
clc
clear all
close all
%% Define value for the parameters
%Mass
Mass=struct('g',9.81,...
    'EU',5,...
    'EL',5,...
    'EB',1,...
    'AL',0,...
    'AU',0,...
    'Load',10);
%lenght
Length=struct('x0',0,'y0',1,...
    'Lb',0.25,...
    'Lu',0.45,...
    'Ll',0.25,...
    'Llow',0.297,...
    'Lupp',0.295);
%Concections
Con=struct('V',0.09,...
    'R',0.075,...
    'omegaY',0.02,...
    'omegaX',-0.02,...
    'LV',0.06,...
    'Lr1',0.05,...
    'Lr1_',0.06,...
    'Lr2',0.10,...
    'LT',0.05,...
    'T',0.083,...
```

```
    'Load',0,...
    'Δ',0.1);

%spring
Spring=struct('k1',0*4.6079e+04,...
    'L01',0.088,...
    'PL1',0.2,...
    'PB1',0.1,);

%Number of points in the plot in both directions
step=25;

Par=struct('Mass',Mass,...
    'Spring',Spring,...
    'Length',Length,...
    'Con',Con,...
    'step',step);
%% Range of motion
l_range=linspace(0,pi/2,step);
u_range=linspace(-pi/2,-pi/4,step);
ll_range=repmat(l_range,step,1);
uu_range=repmat(u_range',1,step);
%% Calculated the energy
[Em,Es,Ls,Pos]=energy_cal(Par,ll_range,uu_range);
t=Em.EU+Em.EL+Em.EB+Em.AL+Em.AU+Em.Load+Es.V1+Es.TV1+Es.V2+Es.V3;
save Runner_data.mat
```

```
function [Em,Es,Ls,Positie]=energy_cal(Par,ELsigma,EUsigma)
%% Calculaed the value of the positions and energy of the exoskeleton
[phiV,phiR]=...
    fourbar(Par.Con.Lr1,Par.Con.LV,Par.Con.V,Par.Con.R,ELsigma);
%angles
phi1=EUsigma;
phi2=ELsigma+EUsigma;
phi3=phi2+phiR;
phi4=phi1+phiV;
%positions
EU1=[Par.Length.x0,Par.Length.y0];
EU2x=EU1(1)+Par.Length.Lu*cos(phi1);
EU2y=EU1(2)+Par.Length.Lu*sin(phi1);

EUTx=EU1(1)+Par.Con.LT*cos(phi1);
EUTy=EU1(2)+Par.Con.LT*sin(phi1);

EL1x=EU2x;
EL1y=EU2y;
EL2x=EL1x+Par.Length.Ll*cos(phi2);
EL2y=EL1y+Par.Length.Ll*sin(phi2);

ELR1x=EL1x+Par.Con.Lr1*cos(phi2);
ELR1y=EL1y+Par.Con.Lr1*sin(phi2);
ELR2x=ELR1x+Par.Con.Lr2*cos(phi2);
ELR2y=ELR1y+Par.Con.Lr2*sin(phi2);

EBR1x=ELR1x+Par.Con.R*cos(phi3);
EBR1y=ELR1y+Par.Con.R*sin(phi3);
EBR2x=ELR2x+Par.Con.R*cos(phi3);
EBR2y=ELR2y+Par.Con.R*sin(phi3);

EB1x=EBR1x-Par.Con.Lr1_*cos(phi2);
EB1y=EBR1y-Par.Con.Lr1_*sin(phi2);
EB2x=EB1x+Par.Length.Lb*cos(phi2);
EB2y=EB1y+Par.Length.Lb*sin(phi2);

EUVx=EU2x-Par.Con.LV*cos(phi1);
EUVy=EU2y-Par.Con.LV*sin(phi1);
```

```
40
41  EBVx=EUVx+Par.Con.V*cos(phi4);
42  EBVy=EUVy+Par.Con.V*sin(phi4);
43
44  AL1x=EB1x-Par.Con.omegaY*sin(phi2)+Par.Con.omegaX*cos(phi2);
45  AL1y=EB1y+Par.Con.omegaY*cos(phi2)+Par.Con.omegaX*sin(phi2);
46  AL2x=AL1x+Par.Length.Llow*cos(phi2);
47  AL2y=AL1y+Par.Length.Llow*sin(phi2);
48
49  Ldx=AL2x-Par.Con.Load*cos(phi2);
50  Ldy=AL2y-Par.Con.Load*sin(phi2);
51
52  Delta=(Par.Con.R*sin(phiR));
53
54  PS1x1=EL1x+Par.Spring.PL1*cos(phi2);
55  PS1y1=EL1y+Par.Spring.PL1*sin(phi2);
56  PS1x2=EB1x+Par.Spring.PB1*cos(phi2);
57  PS1y2=EB1y+Par.Spring.PB1*sin(phi2);
58
59  %Spring lenght
60  Lv1=sqrt((PS1x1-PS1x2).^2+(PS1y1-PS1y2).^2);
61  Uv1=Lv1-Par.Spring.L01;
62  Ls=struct('Lv1',Lv1,'Uv1',Uv1);
63  %% tussenstap
64  %Detimening value for the second four-bar mechanism.
65  x=(AL1x-EL1x);
66  y=(AL1y-EL1y);
67  lamda=sqrt(x.^2+y.^2);
68  alpha=(atan(y./x)-(phi1));
69  % atan y/x is the same for a positive and negastive x so the secting makes
70  % sure that a distication is made.
71  test=find(x>0);
72  sizetest=size(test);
73  if sizetest(1) == 0
74      alpha=pi+alpha;
75  elseif sizetest(1) == Par.step
76       alpha=alpha+pi;
77  else
78      Trans=find(x<0);
79      alpha(test)=(alpha(test)-pi);
80      alpha=pi-alpha;
81  end
82  TtoV=(Par.Length.Lu-Par.Con.LT);
83  %% Calculaed the value of the positions and energy of the user
84  [phiT,Ephi,error2]=...
85      fourbar(lamda,TtoV,Par.Con.T,Par.Length.Lupp,(alpha+pi));
86  phi5=phi1+phiT;
87  AUTx=EUTx+Par.Con.T*cos(phi5);
88  AUTy=EUTy+Par.Con.T*sin(phi5);
89  AU1x=AUTx;
90  AU1y=AUTy;
91
92  X=(AL1x-AU1x);
93  Y=(AU1y-AL1y);
94  AUnu=atan(X./Y)-pi/2;
95  phi6=EUsigma+AUnu;
96  AU2x=AU1x+Par.Length.Lupp*cos(AUnu);
97  AU2y=AU1y+Par.Length.Lupp*sin(AUnu);
98  %% Step to calaculet the resulting moment at the human elbow
99  epson=-AUnu+phi2;
100 %% Setting all the calculated data in one structe array.
101  Positie=struct('EU1',EU1,...);
102     'EU2x',EU2x,'EU2y',EU2y,...
103     'EUTx',EUTx,'EUTy',EUTy,...
104     'EL1x',EL1x,'EL1y',EL1y,...
105     'EL2x',EL2x,'EL2y',EL2y,...
106     'ELR1x',ELR1x,'ELR1y',ELR1y,'ELR2x',ELR2x,'ELR2y',ELR2y,...
```

```
    'EBR1x',EBR1x,'EBR1y',EBR1y,'EBR2x',EBR2x,'EBR2y',EBR2y,...
    'EB1x',EB1x,'EB1y',EB1y,...
    'EB2x',EB2x,'EB2y',EB2y,...
    'EUVx',EUVx,'EUVy',EUVy,...
    'EBVx',EBVx,'EBVy',EBVy,...
    'AL1x',AL1x,'AL1y',AL1y,...
    'AL2x',AL2x,'AL2y',AL2y,...
    'AUTx',AUTx,'AUTy',AUTy,...
    'AU1x',AU1x,'AU1y',AU1y,...
    'AU2x',AU2x,'AU2y',AU2y,...
    'Ldx',Ldx,'Ldy',Ldy,...
    'phiR',phiR,...
    'Ephi',Ephi,...
    'phiV',phiV,...
    'Lv1',Lv1,'Lv3',Lv3,...
    'PS1x1',PS1x1,'PS1y1',PS1y1,'PS1x2',PS1x2,'PS1y2',PS1y2,...
    'Delta',Delta,'alpha',alpha,'x',x,'y',y,'phiT',phiT,'AUnu',AUnu,...
    'phi2',phi2,'epson',epson,'error',error,'phi1',phi1,...
    'phi3',phi3,'phi4',phi4,'phi5',phi5);
%% Defining the potential energy of the exoskeleton
energyEU=Par.Mass.g*Par.Mass.EU*(EU1(2)+0.5*Par.Length.Lu*sin(phi1));
energyEL=Par.Mass.g*Par.Mass.EL*(EL1y+0.5*Par.Length.Ll*sin(phi2));
energyEB=Par.Mass.g*Par.Mass.EB*(EB1y+0.5*Par.Length.Lb*sin(phi2));
energyAL=Par.Mass.g*Par.Mass.AL*(AL1y+0.5*Par.Length.Llow*sin(phi2));
energyAU=Par.Mass.g*Par.Mass.AU*(AUTy+0.5*Par.Length.Lupp*sin(phi6));
energyLd=Par.Mass.g*Ldy*Par.Mass.Load;
Em=struct('EU',energyEU,'EL',energyEL,'EB',energyEB,'AL',energyAL,...
    'AU',energyAU,'Load',energyLd);
%spring
energyV1=0.5*Par.Spring.k1*Uv1.^2;
Es=struct('V1',energyV1));
```

```
function [phiV,phiR] = fourbar(a,b,c,d,beta)
phi=2*pi-beta;
R1=a./d; R2=a./b; R3=(a.^2+b.^2-c.^2+d.^2)./(2.*b.*d);
A=(1-R2).*cos(phi)+R3-R1;
B=-sin(phi)*2;
C=-(1+R2).*cos(phi)+R3+R1;
x= (-B-sqrt(B.^2-4.*A.*C))./(2.*A);
phiV=pi-atan(x)*2;
lamda=(b.*cos(phiV)-a).^2+(b*sin(phiV)).^2;
phiR=acos((c.^2+d.^2-lamda)./(2*c.*d));
```

```
function [phiV,phiR] = fourbar2(a,b,c,d,beta)
phi=2*pi-beta;
R1=a./d; R2=a./b; R3=(a.^2+b.^2-c.^2+d.^2)./(2.*b.*d);
A=(1-R2).*cos(phi)+R3-R1;
B=-sin(phi)*2;
C=-(1+R2).*cos(phi)+R3+R1;
x= (-B-sqrt(B.^2-4.*A.*C))./(2.*A);
phiV=pi-atan(x)*2;
lamda=(b.*cos(phiV)-a).^2+(b*sin(phiV)).^2;
phiR=acos((c.^2+d.^2-lamda)./(2*c.*d));
```

Appendix D

Force analysis

Figure D.1 shows an exploded view of the design. Figure D.2 shows all the points used to define the positions and lengths. It is addressed in the paper that there are no forces in points O and P. This implies that there are no force on body 1.
Body 2 has four forces acting on it where the F_{load} is know.

$$F_{load:x2} = F_{load} \sin\theta \tag{D.1}$$
$$F_{load:y2} = F_{load} \cos\theta \tag{D.2}$$

Addressing the forces in the x_2 direction.

$$\sum F_{x2} = 0 \tag{D.3}$$
$$F_{V:x2} = F_{load:x2} \tag{D.4}$$

$$b_x = -F_{V:x_2} \cos\theta_2 \tag{D.5}$$
$$b_y = -F_{V:x_2} \sin\theta_2 \tag{D.6}$$

Calculating the F_V and $F_{V:y2}$ a set or linear equations is used (see Fig. D.3). $\varphi_{V:g}$ is the φ_V with respect to the global reference plane.

$$x = A^{-1}\mathbf{b} \tag{D.7}$$

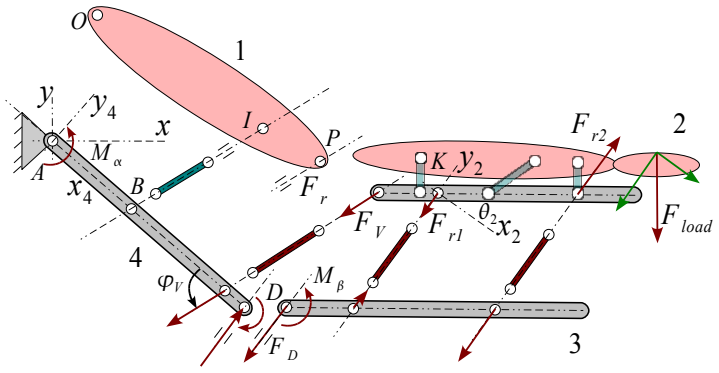

Figure D.1: Free body diagram of the design without the spring.

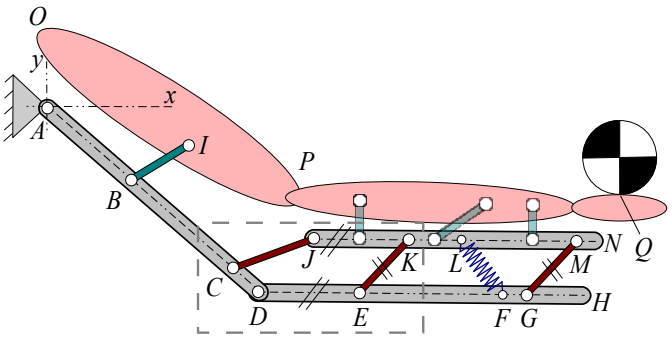

Figure D.2: Schematic representation of the final concept with all points indicated.

where

$$A = \begin{bmatrix} \cos\varphi_{V:g} & -\cos\theta_2 \\ \sin\varphi_{V:g} & -\sin\theta_2 \end{bmatrix} \tag{D.8}$$

$$\mathbf{b} = \begin{bmatrix} -F_{V:x_2}\cos\theta_2 \\ -F_{V:x_2}\sin\theta_2 \end{bmatrix} \tag{D.9}$$

$$\mathbf{x} = \begin{bmatrix} F_V \\ F_{V:y2} \end{bmatrix} \tag{D.10}$$

Selecting the moment around point K.

$$\sum M_K = 0 \tag{D.11}$$

$$F_{V:y2}\cdot|JK| + F_{r2}\cdot|KM| + F_{load:y2}\cdot|JQ| = 0 \tag{D.12}$$

$$-\frac{F_{V:y2}\cdot|JK| - F_{load:y2\cdot|JQ|}}{|KM|} = F_{r2} \tag{D.13}$$

Taking the sum of all froces in the y_2 direction the last force can be calculated.

$$\sum F_y 2 = 0 \tag{D.14}$$

$$F_{V:y2} + F_{r1} + F_{r2} + F_{load:y2} = 0 \tag{D.15}$$

$$-F_{V:y2} - F_{r2} - F_{load:y2} = F_{r1} \tag{D.16}$$

There are three forces and one moment (M_β) acting on body 3.

$$\sum F_{y_2} = 0 \tag{D.17}$$

$$F_D + F_{r1} + F_{r2} = 0 \tag{D.18}$$

$$-F_{r1} - F_{r2} = F_D \tag{D.19}$$

To find a moment equilibrium M_β must counteract the moment exerted by F_{r1} and F_{r2}. To determine the resulting moment the local force vector perpendicular to the body must be calculated.

$$F_{r1:y} = F_{r1}\cos\varphi_r \tag{D.20}$$

$$F_{r2:y} = F_{r2}\cos\varphi_r \tag{D.21}$$

With the two acting force the moment is calculated around point D.

$$\sum M_D = 0 \tag{D.22}$$

$$F_{r1:y}\cdot|DE| + F_{r2:y}\cdot|DF| + M_\beta = 0 \tag{D.23}$$

$$-F_{r1:y}\cdot|DE| - F_{r2:y}\cdot|DF| = M_\beta \tag{D.24}$$

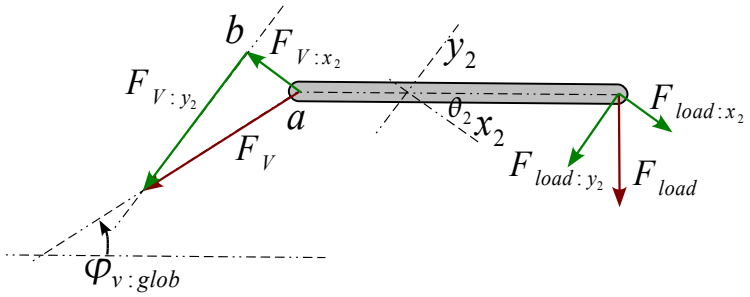

Figure D.3: Detailed schematic representation of body 1 to illustrated the calculation of F_V

Body 4 is the last body where the equilibrium must be calculated.

$$F_{V:y_4} = F_V \sin \varphi_V \tag{D.25}$$
$$F_{V:x_4} = F_V \cos \varphi_V \tag{D.26}$$

To determine the longitudinal and perpendicular force of F_D the relative angle must be expressed (φ_D).

$$\varphi_D = \beta + \varphi_r \tag{D.27}$$
$$F_{D:y_4} = F_D \sin \varphi_D \tag{D.28}$$
$$F_{D:x_4} = F_D \cos \varphi_D \tag{D.29}$$

The three equilibrium are calculated. The forces is the y_4 direction.

$$\sum F_{y_4} = 0 \tag{D.30}$$
$$F_{D:y_4} + F_{V:y_4} + F_{a:y_4} = 0 \tag{D.31}$$
$$-F_{D:y_4} - F_{V:y_4} = F_{a:y_4} \tag{D.32}$$

The Forces in the x_4 direction.

$$\sum F_{x_4} = 0 \tag{D.33}$$
$$F_{D:x_4} + F_{V:x_4} + F_{a:x_4} = 0 \tag{D.34}$$
$$-F_{D:x_4} - F_{V:x_4} = F_{a:x_4} \tag{D.35}$$

The moment around point a.

$$\sum M_a = 0 \tag{D.36}$$
$$M_\beta + F_{V:y_4} \cdot |AC| + F_{D:y_4} \cdot |AD| + M_\alpha = 0 \tag{D.37}$$
$$-F_{V:y_4} \cdot |AC| - F_{D:y_4} \cdot |AD| - M_\alpha = M_\beta \tag{D.38}$$

Appendix E

Prototype

This appendix addresses the demonstrator in more detail.

E.1 Dimension

The design parameters are listed in Tab. F.3. There are two types of joints created.

Table E.1: Parameters of the demonstrator

Parameter	Quantity	Unit	Material	Size	Unit
$\|AD\|$	0.3	m	wood	0.021×0.029	m
$\|AB\|$	0.049	m	-	-	-
$\|BI\|$	0.083	m	aluminium	0.003×0.026	m
$\|CD\|$	0.06	m	-	-	-
$\|CJ\|$	0.09	m	aluminium	0.003×0.026	m
$\|DH\|$	0.25	m	wood	0.021×0.029	m
$\|DE\|$	0.05	m	-	-	-
$\|EF\|$	0.15	m	-	-	-
$\|EK\|$	0.075	m	aluminium	0.003×0.026	m
$\|JK\|$	0.06	m	-	-	-
$\|JN\|$	0.25	m	steel	0.004×0.02	m

Table E.2: Bolts used as joints

Joints	B, C, D, E, G		J, K, M	
	M8 × 40	[mm]	M5 × 16	[mm]

E.2 Photos

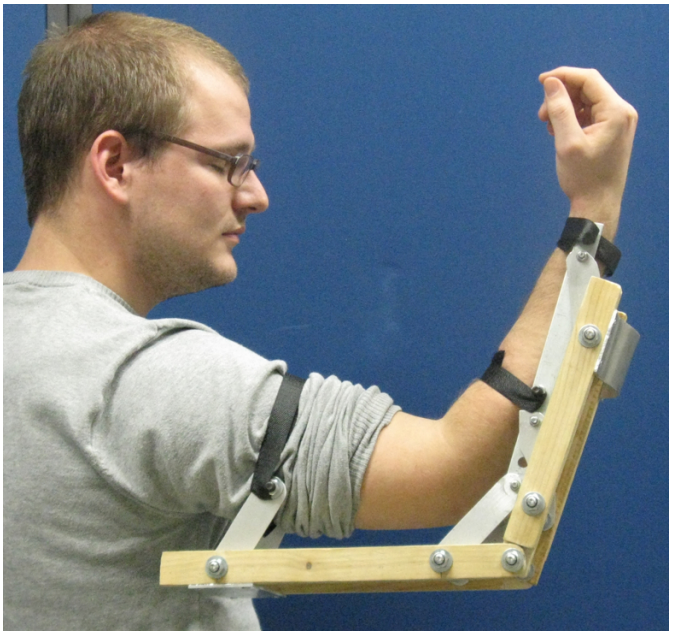

Figure E.1: Photo of the demonstrator in fully flexed position.

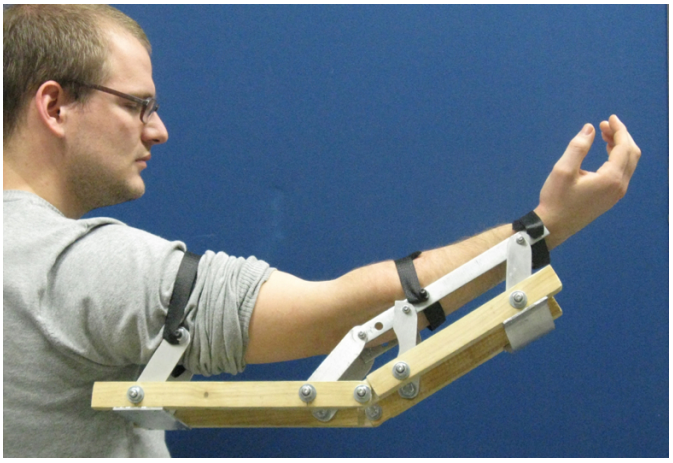

Figure E.2: Photo of the demonstrator in between extension and flex position.

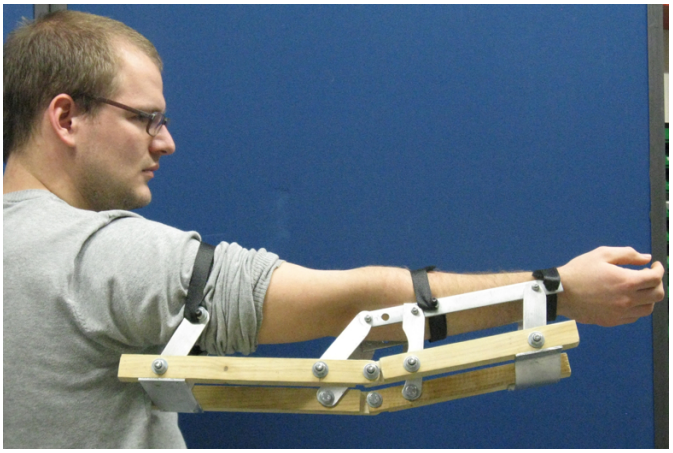

Figure E.3: Photo of the demonstrator in fully extended position.

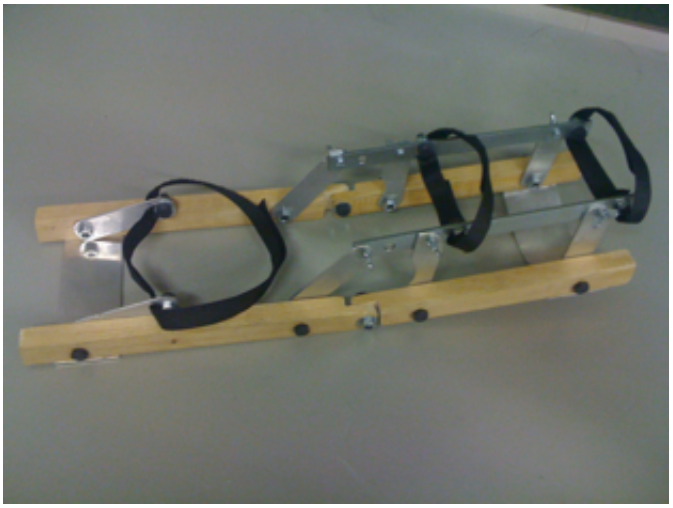

Figure E.4: Photo of the demonstrator.

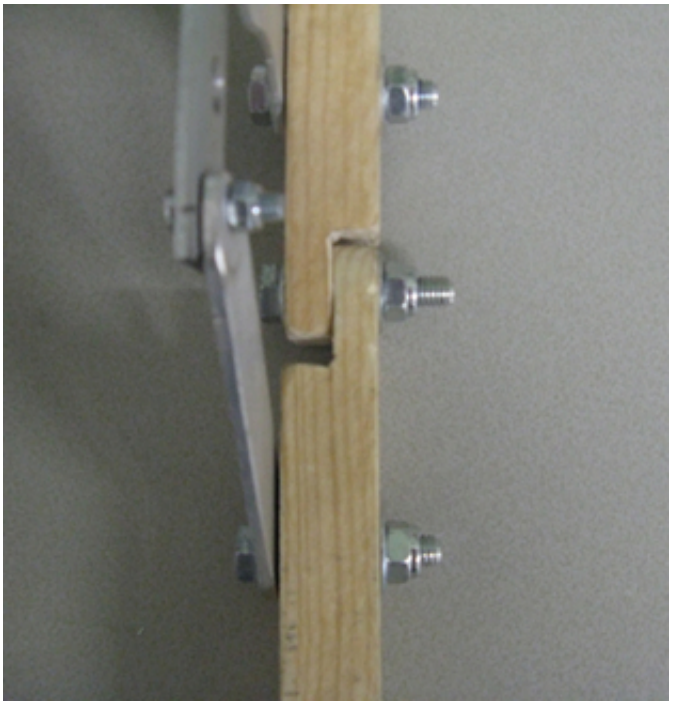

Figure E.5: Photo of the demonstrator the main joint of the exoskeleton.

Appendix F

Optimalisation of test setup

To achieve a good gravity compensation an optimization is done. The following design vector is chosen. The corresponding points are indicated in Fig F.1. Table F.1 list the design space for the design vector.

$$\mathbf{s} = [|CJ|, k, l_{k0}, |JK|, |DF|] \tag{F.1}$$

To achieve the optimization goal a fitness function is formulated. Equation F.2 shows the fitness function. The moment M_β is acting on the joint indicated by point D. $\bar{M}_\beta$ and $\bar{E}_p$ are the main values of the corresponding moment and potential energy.

$$\min_{\mathbf{s}} \left(\lambda_1 \cdot f_{M_\beta}(\mathbf{s}) + \lambda_2 \cdot f_{E_p}(\mathbf{s})\right) \tag{F.2}$$

where

$$f_{M_\beta}(\mathbf{s}) = \int_0^{\frac{\pi}{2}} \left[M_\beta(\mathbf{s}, \beta) - \bar{M}_\beta(\mathbf{s})\right]^2 d\beta \tag{F.3}$$

$$f_{E_p}(\mathbf{s}) = \int_0^{\frac{\pi}{2}} \left[E_p(\mathbf{s}, \beta) - \bar{E}_p(\mathbf{s})\right]^2 d\beta \tag{F.4}$$

The function is constructed out of two sub function. Sub function f_{M_β} relates to the moment M_β. The sub function f_{E_p} relate to the potential energy change in the system. Two weight factors λ_1, λ_2 are used combine these sub functions.

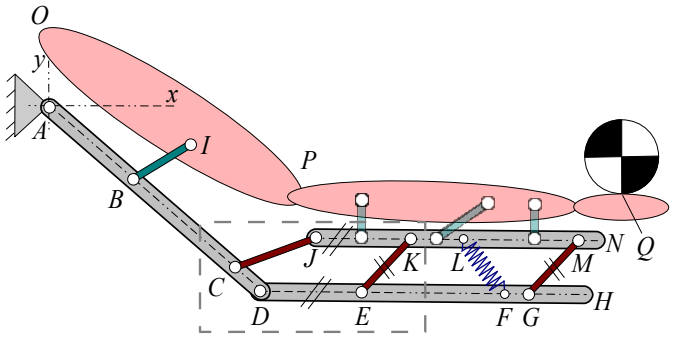

Figure F.1: Schematic representation of the final concept with all points indicated.

Table F.1: The design space for the design vector.

Parameter	Minimum	Maximum	Unit
$\|CJ\|$	0.03	0.09	m
k	1000	10000	$\frac{N}{m}$
L_{k0}	0	0.12	m
$\|JK\|$	0.05	0.07	m
$\|DF\|$	0	0.25	m

Table F.2: Masses used for the optimization

Parameter	Quantity	Unit
m_l	2	kg
m_b	1.5	kg
m_{load}	10	kg

There are two evaluation criteria used which are based on the moment with the optimized gravity compensation M_{opti}.

$$\Delta_E = 100 - \frac{\max|M_{opti}|}{\max|M_\beta|} \cdot 100[\%] \tag{F.5}$$

$$\Delta_M = 100 - \frac{\max|M_{opti}| - \min|M_{opti}|}{\max|M_\beta| - min|M_\beta|} \cdot 100[\%] \tag{F.6}$$

The potential energy in the system depends on the masses of the system. The masses were estimated and are listed in Tab. F.2. The design parameters are chosen and are listed in Tab. F.3.

Table F.3: Parameters of analytical model and the demonstrator

Parameter	Quantity	Unit
$\|AD\|$	0.3	m
$\|AB\|$	0.049	m
$\|BI\|$	0.083	m
$\|CD\|$	0.06	m
$\|CJ\|$	0.09	m
$\|DH\|$	0.25	m
$\|DE\|$	0.05	m
$\|EF\|$	0.15	m
$\|EK\|$	0.075	m
$\|JK\|$	0.06	m
$\|JN\|$	0.25	m

Table F.4: Parameters output from the optimization for different values for λ_1 and λ_2.

$\lambda_1 = 3 \quad \lambda_2 = 1$

Parameter	Quantity	Unit
$\|CJ\|$	0.0522	m
k	2392	$\frac{N}{m}$
L_{k0}	0.0469	m
$\|JK\|$	0.0505	m
$\|DF\|$	0.2108	m
Δ_E	96	%
Δ_M	90	%

$\lambda_1 = 1 \quad \lambda_2 = 3$

Parameter	Quantity	Unit
$\|CJ\|$	0.0505	m
k	2666	$\frac{N}{m}$
L_{k0}	0.0435	m
$\|JK\|$	0.0512	m
$\|DF\|$	0.189	m
Δ_E	95	%
Δ_M	83	%

$\lambda_1 = 1 \quad \lambda_2 = 0$

Parameter	Quantity	Unit
$\|CJ\|$	0.039	m
k	6202	$\frac{N}{m}$
L_{k0}	0.0488	m
$\|JK\|$	0.0518	m
$\|DF\|$	0.0673	m
Δ_E	58	%
Δ_M	96	%

$\lambda_1 = 0 \quad \lambda_2 = 1$

Parameter	Quantity	Unit
$\|CJ\|$	0.0467	m
k	3222	$\frac{N}{m}$
L_{k0}	0.027	m
$\|JK\|$	0.0548	m
$\|DF\|$	0.1380	m
Δ_E	92	%
Δ_M	64	%

Figure F.2 shows the system without gravity compensation. Figures F.3 to F.6 show the energy and moment with gravity compensation optimized with the corresponding λ_1 and λ_2 values. Table F.4 lists the parameters and the achieved Δ_E and Δ_M.
The results show that λ_1 results in a focus on Δ_M and λ_2 results is a focus on Δ_E. Choosing the weight factors so that the influence of f_{M_β} and f_{E_p} is near equal is the most preferred. This results in the lowest spring constant and the best moment reduction and moment fluctuation reduction.

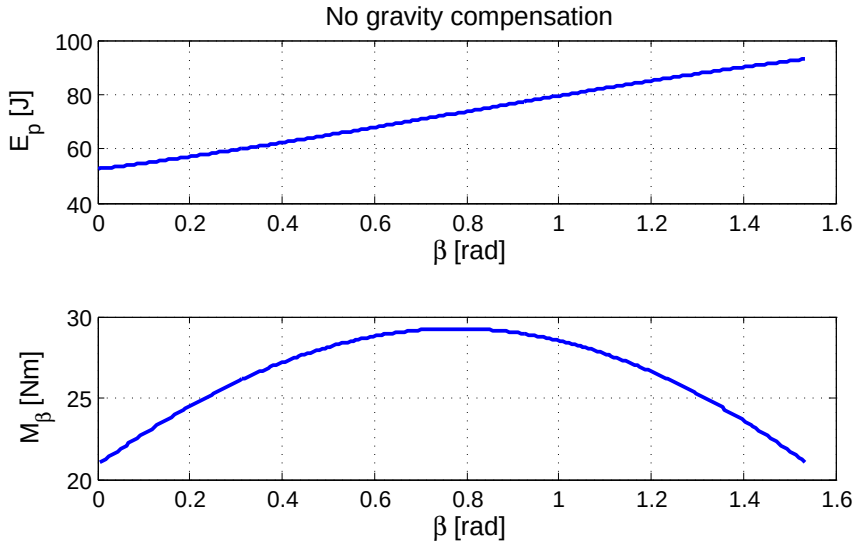

Figure F.2: The energy and the moment around β.

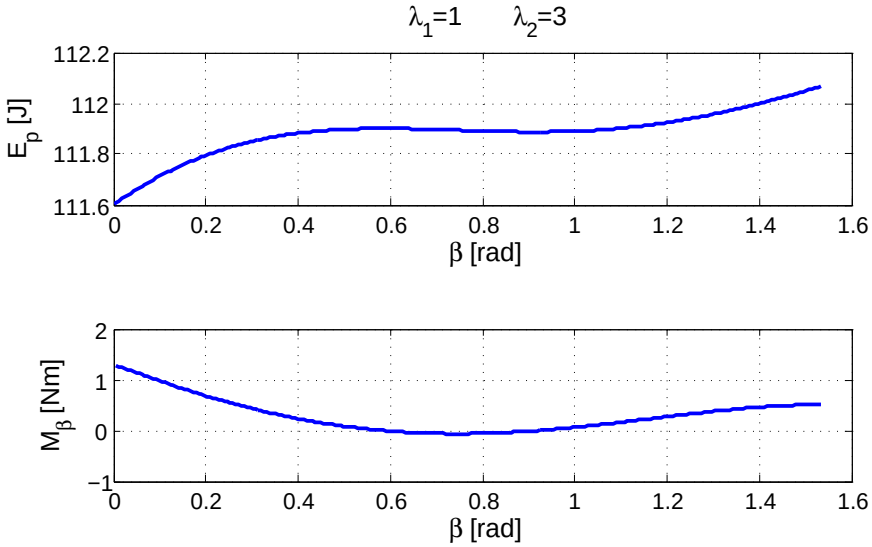

Figure F.3: The energy and the moment around β.

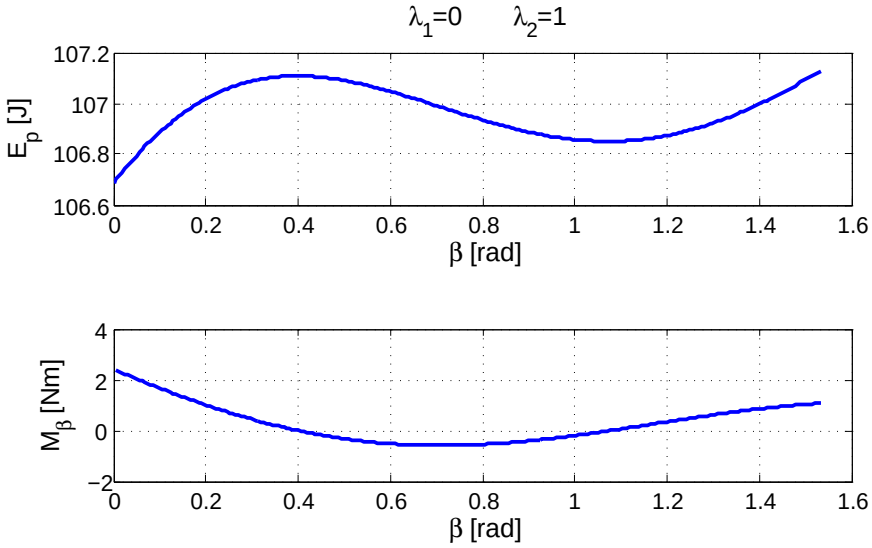

Figure F.4: The energy and the moment around β.

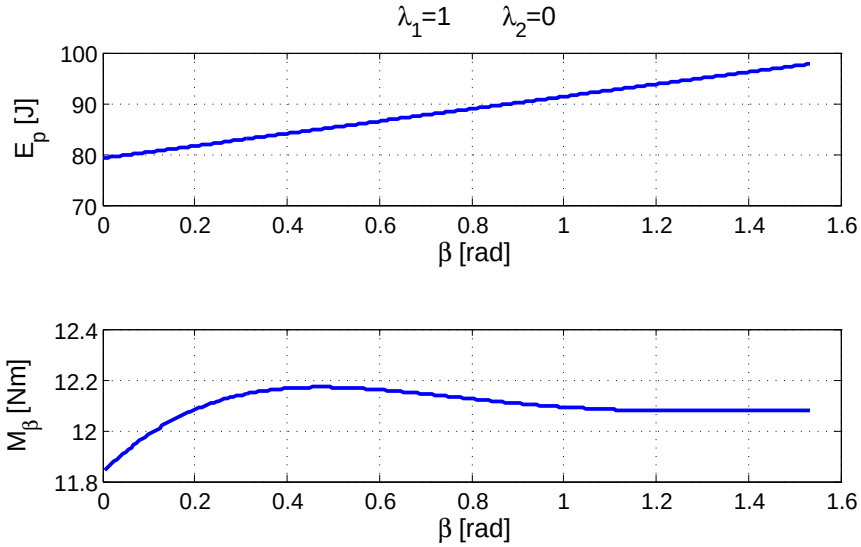

Figure F.5: The energy and the moment around β.

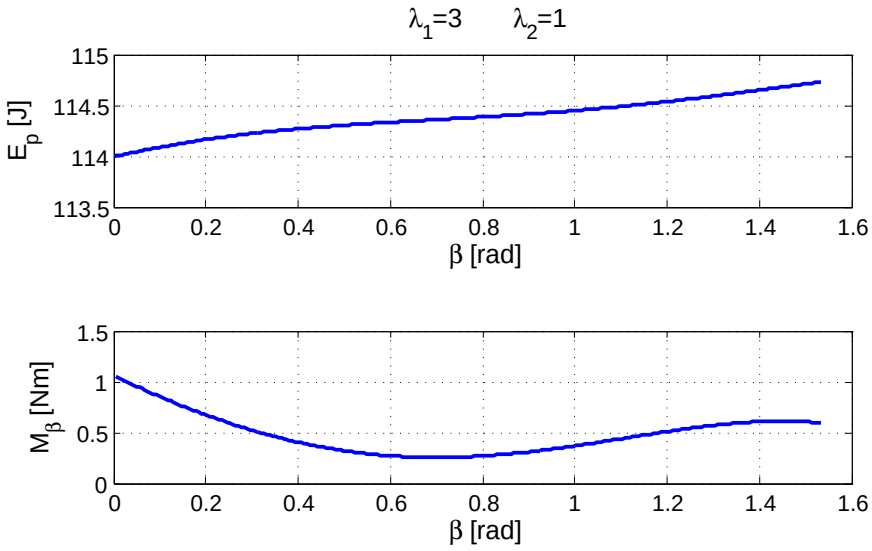

Figure F.6: The energy and the moment around β.

F.1 Matlab code

There are two main .m files that define the optimization.

- **Runner_opti.m**
  This file defines the optimization.
- **Opti_function.m**
  This file defines the finiteness function.

```
%% Runner_opti.m
close all
clear all
clc
%% Defining the parameters
global Mass Length  step l_range u_range
%Mass in [kg]
Mass=struct('g',9.81,...
    'EU',3,...
    'EL',2,...
    'EB',1.5,...
    'AL',0,...
    'AU',0,...
    'Load',40);
%lenght in [m]
Length=struct('x0',0,'y0',0.6,...
    'EB',0.25,...
    'EU',0.3,...
    'EL',0.25,...
    'AL',0.297,...
    'AU',0.295);

step=50;
l_range=linspace(0,pi/2,step);
u_range=linspace(-pi/4,-pi/4,step);
%% Setting for the optimazation
    xl=[0.03  1000  0    0.05 0];
```

```
    xu=[0.09  10000 0.12 0.07 0.25];
    numvar=5;

options = gaoptimset('PopulationSize',575,'TimeLimit',60,...
                     'Generations',50,'PlotFcns',@gaplotbestf);

[x,fval,exit,output] = ga(@Opti_function,numvar,[],[],[],[],xl,xu,[],options);
save x_opti4.mat
Runner
```

```
%% Opti_function.m
function f=Opti_function(x)
%% Define value for the parameters
global Mass Length step l_range u_range
%spring
Spring=struct('k1',x(2),...
    'L01',x(3),...
    'PL1',x(5),...
    'PB1',0);

Con=struct('V',x(1),...
    'R',0.075,...
    'omega',0.02,...
    'omegaX',-0.03,...
    'EUV1',0.06,...
    'ELR1',0.05,...
    'EBR1',x(4),...
    'EBR2',0.05,...
    'EUTL',0.05,...
    'T',0.083,...
    'Load',0,...
    'Δ',0.1);

Par=struct('Mass',Mass,...
    'Spring',Spring,...
    'Length',Length,...
    'Con',Con,...
    'step',step);
%% Calculated the energy
[Em,Es,l,Pos]=energy_cal(Par,l_range,u_range);
t=Em.EU+Em.EL+Em.EB+Em.AL+Em.AU+Em.Load+Es.V1;
td=diff(t',1);
Betad=diff(l_range',1);
Mbeta=td./Betad;
Mmean=mean(mean(Mbeta));
Z=Mbeta-Mmean;
t_mean=mean(mean(t));
Z1=(t-t_mean);
f=4*mean(mean(Z.^2))+1*mean(mean(Z1.^2));
```

Appendix G

Two degree of freedom gravity compensation

There are two main aspects for two degree of freedom gravity compensation

- In the current design there is no gravity compensation for the upper part. The design must include a way to balance the system around the angle α
- The proposed gravity compensation only work for one value of α. The proposed design must be altered to include the angle α.

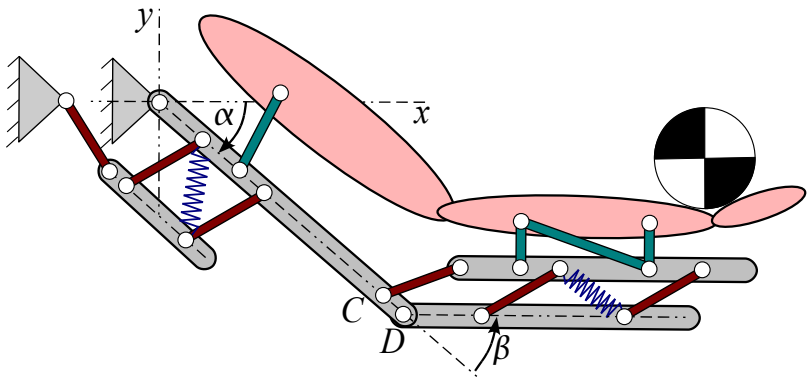

Figure G.1: Schematic representation of 2 degree of freedom gravity compensation.

Figure G.1 shows an additional linkage mechanism. This mechanism used a spring to compensate the gravity for DoF α. The working principle of the system is equal to the lower arm.
Adjusting $|CD|$ with a predetermined relation to α will lead to 2 DoF gravity compensation. The optimization used is adjusted to find the corresponding $|CD|$ for each α. This is done by repeating a optimization loop. The range of α is set is a number of steps. For each step the optimal $|CD|$ is determined for the full range of β. Figure G.2 shows the resulting relationship.

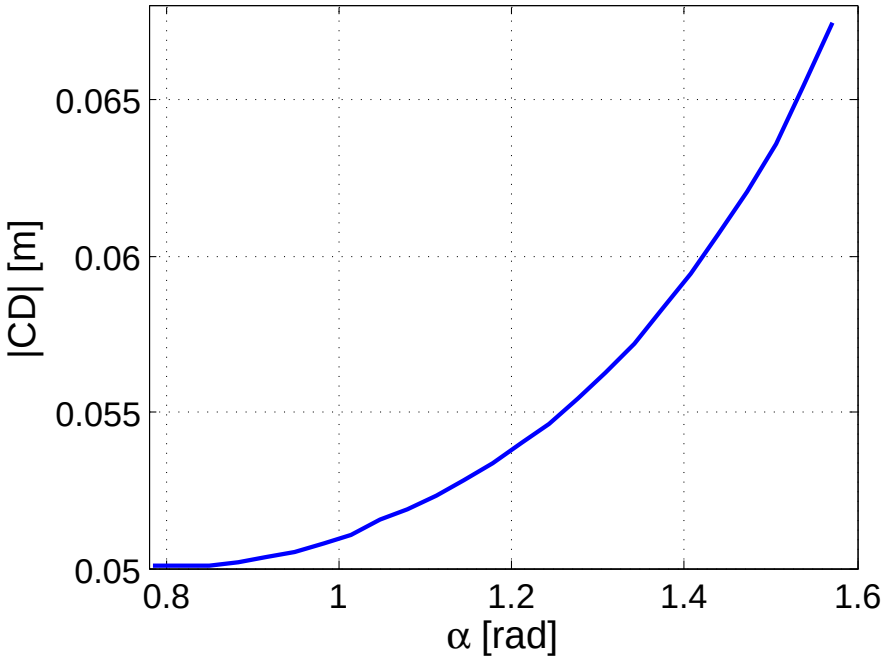

Figure G.2: The relationship between the length $|CD|$ and the angle α